European Journal of Life Sciences

Volume: 1 • Issue: 1 • April 2022 • ISSN: 2822-5333

ANADOLU UNIVERSITY
INSTITUTE OF HEALTH SCIENCES

ANADOLU UNIVERSITY
INSTITUTE OF HEALTH SCIENCES

European Journal of Life Sciences

Volume: 1 • Issue: 1 • April 2022

ISSN: 2822-5333

European Journal of Life Sciences

Owner of the Journal on behalf of Anadolu University
Prof. Dr. Fuat Erdal

Editor in Chief
Prof. Dr. Gülşen Akalın Çiftçi

Editors
Prof. Dr. Yavuz Bülent Köse
Prof. Dr. Gökalp İşcan
Assoc. Prof. Dr. Mustafa Sinan Kaynak
Assoc. Prof. Dr. Hale Gamze Ağalar

Publication Type
International peer-reviewed journal

Publication Frequency
Triannually

Language
English

Website
https://dergipark.org.tr/ejls

Publisher
Anadolu University Institute of Health Sciences

Publisher Address
Anadolu University, Institute of Health Sciences, Yunus Emre Campus, 26470 Tepebaşı/Eskişehir.
Phone: +90 222 320 76 51
E-mail: sagens@anadolu.edu.tr
Web: https://sbe.anadolu.edu.tr/en

Publishing Services
Akdema Informatics, Publishing, and Consultancy Trade LLC
Address: Kızılay Mahallesi, Gazi Mustafa Kemal Bulvarı No: 23/8, 06420 Çankaya/Ankara
E-mail: bilgi@akdema.com
Phone: +90 533 166 80 80
Web site: www.akdema.com

European Journal of Life Sciences

Editorial Board

European Journal of Life Sciences

Contents

ANADOLU UNIVERSITY
INSTITUTE OF HEALTH SCIENCES

European Journal of Life Sciences 2022; 1: 1-7

Research Article

Synthesis and characterization of new piperazine-dithiocarbamate compounds as potent MAO-A inhibitors

Derya Osmaniye[1], Begüm Nurpelin Sağlık[1], Serkan Levent[1], Yusuf Özkay[1], Zafer Asım Kaplancıklı✉[1]

[1]Anadolu University, Faculty of Pharmacy, Department of Pharmaceutical Chemistry, Eskişehir, Turkey.

✉ Zafer Asım Kaplancıklı
zakaplan@anadolu.edu.tr

https://doi.org/10.55971/EJLS.1089254

Received: 03.17.2022
Accepted: 04.08.2022
Available online: 06.06.2022

ABSTRACT

Monoamine oxidase (MAO) enzymes have an important place in neurodegenerative diseases. While MAO-A inhibitors are used in depression; MAO-B enzyme has an important place in Parkinson's disease. Within the scope of this study, 7 new piperazine-dithiocarbamate derivative compounds were synthesized. Structure determinations of the compounds were performed using ^{1}H-NMR, ^{13}C-NMR and HRMS spectroscopic methods. The MAO inhibitory activities of the compounds were determined by *in vitro* fluorometric methods. According to the obtained results, compound **2d** with IC_{50}=0.108±0.004 µM; compound **2e** exhibited inhibitory activity with an IC_{50}=0.074±0.003 µM.

Keywords: Dithiocarbamate, HRMS, Monoamine oxidase, NMR, Piperazine

1. INTRODUCTION

Monoamine oxidase (MAO), an intracellular flavoenzyme in the outer mitochondrial membrane, is responsible for the oxidative deamination of dietary amines, monoamine neurotransmitters and hormones [1,2]. Inhibitors of monoamine oxidases (MAOIs), a member of a protein family of flavin-containing amine oxidoreductases that play an important role in the regulation and metabolism of various neurotransmitters, may be useful in the treatment of psychiatric and neurological diseases [3]. Two MAO isoforms encoded by separate genes and localized to the outer membranes of the mitochondria are termed MAO-A and MAO-B [4]. These isoforms have highly conserved structures. However, the two isozymes have different substrate and inhibitor specificities due to the difference in inhibitor specificities of a pair of gating residues due to a difference in a pair of gating residues [5]. The two isoforms of MAO are dependent on substrate specificity and inhibitor selectivity based on their amino acid sequences, their three-dimensional structure. MAO-A and MAO-B have similar amino acid residues and orientations in their active sites, with only six of the sixteen active site residues differing between the two isozymes. In reality, structural analyses have revealed that MAO-A has a single Å3 550 cavity, but MAO-B has a tighter and longer dipartite cleft known as the entrance and substrate cavities. These two pockets can Å3 unite into a single ~700 cavity [6-8]. Both the MAO-A and -B are present in the majority areas of brain [9]. The MAO-A isoform's substrate specificity includes larger endogenous amines such as norepinephrine, serotonin, and epinephrine, whereas the MAO-B isoform's substrate specificity includes small amines such as β -phenyl ethylamine and benzylamine [10].

There are two types of MAOIs that are used for medicinal purposes nowadays. MAO-A inhibitors are mostly used to treat mental illnesses such as depression and anxiety, whereas MAO-B inhibitors are used to treat Parkinson's and Alzheimer's disease

[11]. Monoaminoxidase inhibitors can reduce peroxide production, which increases neuronal damage and causes nervous system diseases such as Alzheimer's and Parkinson's disease. Monoaminoxidase inhibitors have been used in the treatment of nervous disease [12]. Because central serotonin deficiency and to a lesser extent norepinephrine play a role in depressive illness, MAO-A inhibitors are used as antidepressant agents [13]. WHO predicts that by 2020, depression will be the second most disabling condition in the world, after stress and cardiovascular system [9,14].

Although some MAO-A inhibitors, including phenelzine, isocarboxazid, tranylcypromine, iproniazid, moclobemide and toloxatone, tranylcypromine, iproniazid, moclobemide and toloxatone have made significant contributions to the treatment of depression, their clinical use has been limited due to potential adverse effects, food and medication combinations, and the emergence of other pharmacological classes [15]. In reality, MAO-A inhibitors, especially irreversible inhibitors, are used with caution in the clinic due to their potential to produce a possibly fatal hypertensive crisis when taken with tyramine-containing foods [16]. The development of reversible MAO-A inhibitors, on the other hand, eliminates this difficulty because the reversible inhibitor is displaced from MAO-A when substrate concentrations rise, enabling metabolism to occur [17]. Due to a lack of affinity and selectivity for one of the isoforms, the majority of currently used MAO inhibitors cause adverse effects. As a result, more powerful, reversible, and selective MAO-A and MAO-B inhibitors must be developed [18].

In this study, we aim to present the new piperazine derivatives including dithiocarbamate moiety as selective MAO-A inhibitors.

2. MATERIALS AND METHODS

2.1. Chemistry

All of the chemicals were obtained from commercial sources and utilized without further purification. The uncorrected melting points (M.p.) were determined using the Mettler Toledo-MP90 Melting Point System. ^{1}H-NMR spectroscopy (nuclear magnetic resonance) FT-NMR spectrometer Bruker DPX 300; ^{13}C-NMR spectrometer Bruker DPX 75 MHz (Bruker Bioscience, Billerica, MA, USA). ESI was used to record mass spectra on an LCMS-IT-TOF (Shimadzu, Kyoto, Japan).

2.1.1. Synthesis of Sodium 4-(4-fluorobenzyl) piperazine-1-carbodithioate (1).

1-(4-Fluorobenzyl)piperazine (0.05 mol) was dissolved in EtOH (absolute) in presence of NaOH. Carbon disulfide was dissolved in absolute EtOH, and this solution placed in dropping funnel. It was added dropwise to the reaction medium in an ice bath. The precipitated product was filtered, washed with diethyl ether, and dried at the end of the process.

2.1.2. Synthesis of the target compounds (2a-2c)

Sodium 4-(4-fluorobenzyl)piperazine-1-carbodithioate (0.001 mol) and appropriate 2-bromoacetophenone (0.001 mol) was reacted in 20 ml acetone in room temperature. At the end of the reaction, acetone was evaporated under reduced pressure. The precipitated product was filtered, washed with water, dried, and crystallized from ethanol.

*2-oxo-2-phenylethyl 4-(4-fluorobenzyl)piperazine-1-carbodithioate (**2a**)*

Yield: 81 %, ^{1}H-NMR (300 MHz, DMSO-d_6): δ = 2.47 (4H, br.s., piperazine), 3.54 (2H, s, -CH_2-), 4.00 (2H, br.s., piperazine), 4.19 (2H, br.s., piperazine), 4.96 (2H, s, -CH_2-), 7.16 (2H, t, J=8.9 Hz), 7.36 (2H, dd, J_1=5.7 Hz, J_2=8.6 Hz), 7.55 (2H, t, J=7.7 Hz), 7.64-7.67 (1H, m), 8.04 (2H, d, J=7.1 Hz). ^{13}C-NMR (75 MHz, DMSO-d_6): δ = 44.17, 50.30, 51.76, 52.28, 60.72, 115.48 (J=21.01 Hz), 128.67, 128.68, 129.26, 131.36 (J=7.9 Hz), 133.88, 136.72, 161.87 (J=242.6 Hz), 193.25, 194.83. HRMS (m/z): $[M+H]^+$ calcd for $C_{20}H_{21}N_2OFS_2$: 389.1152; found 389.1134.

*2-oxo-2-(p-tolyl)ethyl 4-(4-fluorobenzyl)piperazine-1-carbodithioate (**2b**)*

Yield: 85 %, ^{1}H-NMR (300 MHz, DMSO-d_6): δ = 2.39 (3H, s, -CH_3), 2.47 (4H, br.s., piperazine), 3.53 (2H, s, -CH_2-), 3.99 (2H, br.s., piperazine), 4.19 (2H, br.s., piperazine), 4.93 (2H, s, -CH_2-), 7.16

(2H, t, *J*=8.9 Hz), 7.34-7.39 (4H, m), 7.94 (2H, d, *J*=8.2 Hz). ^{13}C-NMR (75 MHz, DMSO-d_6): δ = 21.66, 44.11, 50.36, 51.70, 52.28, 60.74, 115.47 (*J*=21.1 Hz), 128.79, 129.78, 129.79, 131.34 (*J*=7.8 Hz), 134.19, 144.33, 161.86 (*J*=242.7 Hz), 192.72, 194.87. HRMS (m/z): $[M+H]^+$ calcd for $C_{21}H_{23}N_2OFS_2$: 403.1309; found 403.1284.

*2-(4-methoxyphenyl)-2-oxoethyl 4-(4-fluorobenzyl) piperazine-1-carbodithioate (**2c**)*

Yield: 75 %, ^{1}H-NMR (300 MHz, DMSO-d_6): δ = 2.48 (4H, br.s., piperazine), 3.54 (2H, s, -CH_2-), 3.85 (3H, s, -OCH_3), 3.99 (2H, br.s., piperazine), 4.20 (2H, br.s., piperazine), 4.91 (2H, s, -CH_2-), 7.07 (2H, d, *J*=8.9 Hz), 7.16 (2H, t, *J*=8.9 Hz), 7.37 (2H, dd, J_1=5.8 Hz, J_2=8.4 Hz), 8.02 (2H, d, *J*=8.9 Hz). ^{13}C-NMR (75 MHz, DMSO-d_6): δ = 43.98, 50.22, 51.78, 52.25, 56.08, 60.71, 114.46, 115.49 (*J*=21.1 Hz), 129.50, 131.06, 131.07, 131.39 (*J*=6.7 Hz), 161.88 (*J*=242.9 Hz), 163.78, 191.53, 194.96. HRMS (m/z): $[M+H]^+$ calcd for $C_{21}H_{23}N_2O_2FS_2$: 419.1258; found 419.1238.

*2-(4-cyanophenyl)-2-oxoethyl 4-(4-fluorobenzyl) piperazine-1-carbodithioate (**2d**)*

Yield: 89 %, ^{1}H-NMR (300 MHz, DMSO-d_6): δ = 2.46 (4H, br.s., piperazine), 3.52 (2H, s, -CH_2-), 3.98 (2H, br.s., piperazine), 4.18 (2H, br.s., piperazine), 4.93 (2H, s, -CH_2-), 7.16 (2H, t, *J*=8.9 Hz), 7.36 (2H, dd, J_1=5.7 Hz, J_2=8.6 Hz), 7.62 (2H, d, *J*=8.6 Hz), 8.65 (2H, d, *J*=8.6 Hz). ^{13}C-NMR (75 MHz, DMSO-d_6): δ = 44.02, 50.33, 51.70, 52.18, 60.65, 115.50 (*J*=21.1 Hz), 115.69, 118.62, 129.24, 129.56, 131.43 (*J*=5.3 Hz), 133.31, 140.11, 161.91 (*J*=241.5 Hz), 163.78, 193.05, 194.59. HRMS (m/z): $[M+H]^+$ calcd for $C_{21}H_{20}N_3OFS_2$: 414.1105; found 414.1119.

*2-(4-nitrophenyl)-2-oxoethyl 4-(4-fluorobenzyl) piperazine-1-carbodithioate (**2e**)*

Yield: 80 %, ^{1}H-NMR (300 MHz, DMSO-d_6): δ = 2.46 (4H, br.s., piperazine), 3.52 (2H, s, -CH_2-), 3.98 (2H, br.s., piperazine), 4.17 (2H, br.s., piperazine), 4.97 (2H, s, -CH_2-), 7.16 (2H, T, *J*=8.8 Hz), 7.35 (2H, dd, J_1=6.0 Hz, J_2=8.1 Hz), 8.26 (2H, d, *J*=8.9 Hz), 8.37 (2H, d, *J*=8.9 Hz). ^{13}C-NMR (75 MHz, DMSO-d_6): δ = 44.13, 51.57, 51.91, 52.30, 60.77, 115.45 (*J*=21.1 Hz), 124.37, 130.02, 131.28 (*J*=7.9 Hz), 134.15, 134.20, 141.62, 150.37, 161.83 (*J*=242.7 Hz), 192.93, 194.47. HRMS (m/z): $[M+H]^+$ calcd for $C_{20}H_{20}N_3O_3FS_2$: 434.1003; found 434.1006.

*2-(4-fluorophenyl)-2-oxoethyl 4-(4-fluorobenzyl) piperazine-1-carbodithioate (**2f**)*

Yield: 70 %, ^{1}H-NMR (300 MHz, DMSO-d_6): δ = 2.48 (4H, br.s., piperazine), 3.54 (2H, s, -CH_2-), 3.99 (2H, br.s., piperazine), 4.19 (2H, br.s., piperazine), 4.94 (2H, s, -CH_2-), 7.16 (2H, t, *J*=8.9 Hz), 7.34-7.42 (4H, m), 8.13 (2H, dd, J_1=5.5 Hz, J_2=8.9 Hz). ^{13}C-NMR (75 MHz, DMSO-d_6): δ = 44.03, 50.34, 51.77, 52.26, 60.71, 115.48 (*J*=21.1 Hz), 116.29 (*J*=21.9 Hz), 131.37 (*J*=7.7 Hz), 131.69 (*J*=9.5 Hz), 133.47, 133.50, 161.87 (*J*=242.78 Hz), 165.55 (*J*=251.9 Hz), 191.94, 194.77. HRMS (m/z): $[M+H]^+$ calcd for $C_{20}H_{20}N_2OF_2S_2$: 407.1058; found 407.1039.

*2-(4-chlorophenyl)-2-oxoethyl 4-(4-fluorobenzyl) piperazine-1-carbodithioate (**2g**)*

Yield: 80 %, ^{1}H-NMR (300 MHz, DMSO-d_6): δ = 2.46 (4H, br.s., piperazine), 3.52 (2H, s, -CH_2-), 3.98 (2H, br.s., piperazine), 4.18 (2H, br.s., piperazine), 4.93 (2H, s, -CH_2-), 7.16 (2H, t, *J*=8.9 Hz), 7.33-7.38 (2H, m), 7.63 (2H, d, *J*=8.6 Hz), 8.06 (2H, d, *J*=8.6 Hz). ^{13}C-NMR (75 MHz, DMSO-d_6): δ = 43.98, 50.49, 51.88, 52.31, 60.78, 115.46 (*J*=21.1 Hz), 129.37, 130.58, 131.29 (*J*=8.1 Hz), 134.17, 134.21, 135.47, 138.75, 161.83 (*J*=242.7 Hz), 192.46, 194.65. HRMS (m/z): $[M+H]^+$ calcd for $C_{20}H_{20}N_2OFS_2Cl$: 423.0762; found 423.0746.

2.2. MAO Enzymes Inhibition Assay

The in vitro MAO inhibition test was carried out using the standard fluorometric method, and the percentages and IC_{50} values of the compounds obtained were reported as described by our research group already [19-25].

3. RESULTS AND DISCUSSION

3.1. Chemistry

The compounds **2a**-**2g** were obtained as presented in **Scheme 1**. Initially, a sodium 4-(4-fluorobenzyl) piperazine-1-carbodithioate (**1**) was obtained by means of the reaction between 1-(4-fluorobenzyl)

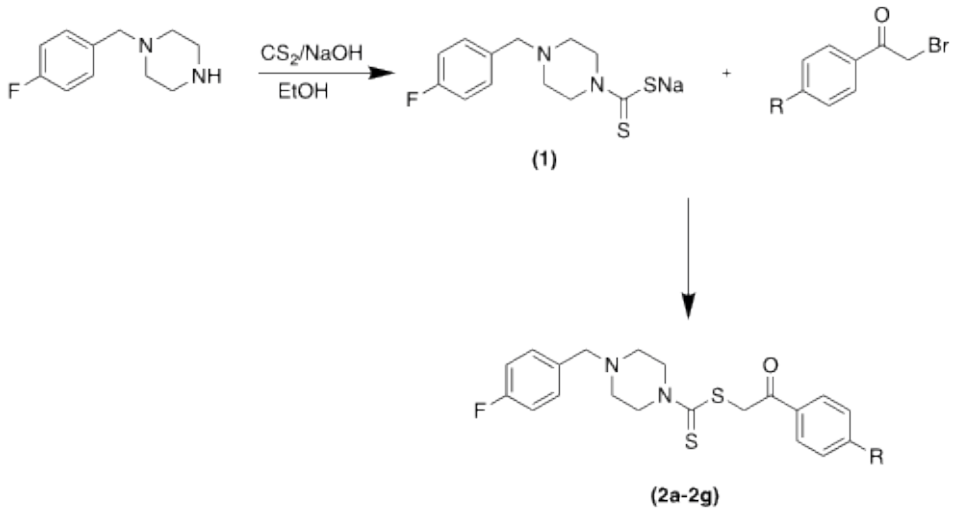

Compounds	R
2a	-H
2b	-CH_3
2c	-OCH_3
2d	-CN
2e	-NO_2
2f	-F
2g	-Cl

Scheme 1. Synthesis pathway for obtained compounds (**2a-2g**)

piperazine and carbon disulfide using NaOH. Secondly, the resulting products were obtained by reacting the sodium 4-(4-fluorobenzyl) piperazine-1-carbodithioate with appropriate 2-bromoacetophenone derivatives. The structures of the compounds obtained were established by spectroscopic methods, namely ^{1}H-NMR, ^{13}C-NMR, and HRMS.

3.2. MAO Enzymes Inhibition Assay

The in vitro fluorometric approach published previously by our research group was used to

Table 1. % Inhibition and IC50 values of the synthesized compounds, moclobemide and selegiline against MAO-A and MAO-B.

Compounds	MAO-A % Inhibition		MAO-A	MAO-B % Inhibition		MAO-B
	10-3 M	10-4 M	IC_{50} (µM)	10-3 M	10-4 M	IC_{50} (µM)
2a	**65.152±1.234**	42.861±0.948	>100	45.451±0.763	24.451±0.632	>1000
2b	**72.647±1.052**	40.542±0.891	>100	41.894±0.612	20.132±0.741	>1000
2c	**68.496±1.319**	46.668±0.961	>100	36.135±0.754	28.648±0.665	>1000
2d	**90.497±1.316**	**84.433±0.868**	**0.108±0.004**	35.532±0.817	27.745±0.662	>1000
2e	**93.134±1.034**	**90.225±0.921**	**0.074±0.003**	33.177±0.793	20.647±0.765	>1000
2f	**63.320±1.263**	41.150±0.918	>100	38.736±0.806	20.349±0.621	>1000
2g	**69.033±0.958**	44.962±0.845	>100	43.940±0.730	31.033±0.733	>1000
Moclobemid	94.121±2.760	82.143±2.691	6.061±0.262	-	-	-
Selegiline	-	-	-	98.258±1.052	96.107±1.165	0.037±0.001

assess the inhibitory capability of the synthesized compounds on MAO isoenzymes [19-25]. % Inhibition and IC_{50} values of the synthesized compounds, moclobemide and selegiline against MAO-A and MAO-B were presented in **Table-1**. As seen in **Table-1**, none of the compounds showed more than 50% inhibition against MAO-B enzyme at 10^{-4} M concentration. In contrast, compounds **2d** and **2e** showed greater than 50% inhibitory activity against the MAO-A enzyme. Therefore, serial dilutions of these compounds at 10^{-3}-10^{-9} M concentrations were prepared and their inhibitory activities on MAO-A enzyme were investigated. According to the results obtained, compound **2d** with IC_{50}=0.108±0.004 µM; compound **2e** exhibited inhibitory activity with an IC_{50}=0.074±0.003 µM.

3.2.1. Statistical analysis

Percentage of % inhibitions compared to the control group and values of IC_{50} were determined. All descriptive data were expressed as the mean±standart error of mean (SEM) from 5 times repetition within the experiments. Data were calculated on Microsoft Excel software with the sigmoidal dose-response curves by using Hill equation.

4. CONCLUSION

MAO-A inhibitors are used in the treatment of depression. However, this group of drugs is not preferred because of their side-effect profiles. Therefore, there is a need for new inhibitors with a reduced side-effect profile. Within the scope of this study, 7 new piperazine-dithiocarbamate derivative compounds were synthesized. Structure determinations of the compounds were performed using ^{1}H-NMR, ^{13}C-NMR and HRMS spectroscopic methods. The MAO inhibitory activities of the compounds were determined by *in vitro* fluorimetric methods. None of the compounds showed inhibitory activity against the MAO-B enzyme. In contrast, compounds **2d** and **2e** showed greater than 50% inhibitory activity against the MAO-A enzyme. According to the obtained results, compound **2d** with IC_{50}=0.108±0.004 µM; compound **2e** exhibited inhibitory activity with an IC_{50}=0.074±0.003 µM. When the structures of the compounds are examined, compound **2d** contains CN group and compound **2e** contains NO_2 group. Both groups are active groups that can withdraw electrons. Therefore, it is thought that such substituents contribute positively to the activity.

ACKNOWLEDGEMENTS

As the authors of this study, we thank Anadolu University Faculty of Pharmacy Central Laboratory for their support and contributions.

Ethical approval

Not applicable, because this article does not contain any studies with human or animal subjects.

Author contribution

Concept: ZAK, YO; Design: ZAK, YO; Supervision: ZAK; Materials: DO, BNS, SL; Data Collection and/or Processing: DO, BNS, SL; Analysis and/or Interpretation: DO, BNS, SL; Literature Search: DO, ZAK; Writing: DO, ZAK; Critical Reviews: YO, ZAK.

Source of funding

This research received no grant from any funding agency/sector.

Conflict of interest

The authors declared that there is no conflict of interest.

REFERENCES

1. Mattsson C, Svensson P, Sonesson C. A novel series of 6-substituted 3-(pyrrolidin-1-ylmethyl) chromen-2-ones as selective monoamine oxidase (MAO) A inhibitors. Eur J Med Chem. 2014;73:177-186. https://doi.org/10.1016/j.ejmech.2013.11.035
2. Choi JW, Jang BK, Cho NC, et al. Synthesis of a series of unsaturated ketone derivatives as selective and reversible monoamine oxidase inhibitors. Bioorg Med Chem. 2015;23(19):6486-6496. https://doi.org/10.1016/j.bmc.2015.08.012

3. He X, Chen YY, Shi JB, et al. New coumarin derivatives: Design, synthesis and use as inhibitors of hMAO. Bioorg Med Chem. 2014;22(14):3732-3738. https://doi.org/10.1016/j.bmc.2014.05.002

4. Baek SC, Lee HW, Ryu HW, et al. Selective inhibition of monoamine oxidase A by hispidol. Bioorg Med Chem Lett. 2018;28(4):584-588. https://doi.org/10.1016/j.bmcl.2018.01.049

5. Baek SC, Kang MG, Park JE, et al. Osthenol, a prenylated coumarin, as a monoamine oxidase A inhibitor with high selectivity. Bioorg Med Chem Lett. 2019;29(6):839-843. https://doi.org/10.1016/j.bmcl.2019.01.016

6. Mostert S, Petzer A, Petzer JP. The evaluation of 1, 4-benzoquinones as inhibitors of human monoamine oxidase. Eur J Med Chem. 2017;135:196-203. https://doi.org/10.1016/j.ejmech.2017.04.055

7. Distinto S, Meleddu R, Yanez M, et al. Drug design, synthesis, in vitro and in silico evaluation of selective monoaminoxidase B inhibitors based on 3-acetyl-2-dichlorophenyl-5-aryl-2, 3-dihydro-1, 3, 4-oxadiazole chemical scaffold. Eur J Med Chem. 2016;108:542-552. https://doi.org/10.1016/j.ejmech.2015.12.026

8. Tong X, Chen R, Zhang TT, Han Y, Tang W-J, Liu XH. Design and synthesis of novel 2-pyrazoline-1-ethanone derivatives as selective MAO inhibitors. Bioorg Med Chem. 2015;23(3):515-525. https://doi.org/10.1016/j.bmc.2014.12.010

9. Suthar SK, Bansal S, Alam MM, et al. Design, synthesis, and biological evaluation of oxindole derivatives as antidepressive agents. Bioorg Med Chem Lett. 2015;25(22):5281-5285. https://doi.org/10.1016/j.bmcl.2015.09.048

10. Manzoor S, Hoda N. A comprehensive review of monoamine oxidase inhibitors as Anti-Alzheimer's disease agents: A review. Eur J Med Chem. 2020;206:112787. https://doi.org/10.1016/j.ejmech.2020.112787

11. Khattab SN, Moneim SAA, Bekhit AA, et al. Exploring new selective 3-benzylquinoxaline-based MAO-A inhibitors: design, synthesis, biological evaluation and docking studies. Eur J Med Chem. 2015;93:308-320. https://doi.org/10.1016/j.ejmech.2015.02.020

12. Hussein FM, Abdulsada SH, Khamis WM, Abdulredha S, Abbas BF. Effect of ferric nanoparticles on monoaminoxidase and acetylcholinesterase in healthy human sera. Asian J Chem. 2018;30(8):1747-1750. https://doi.org/10.14233/ajchem.2018.21284

13. Chirkova ZV, Kabanova MV, Filimonov SI, et al. Inhibition of monoamine oxidase by indole-5, 6-dicarbonitrile derivatives. Bioorg Med Chem Lett. 2015;25(6):1206-1211. https://doi.org/10.1016/j.bmcl.2015.01.061

14. Lewellyn K, Bialonska D, Chaurasiya ND, Tekwani BL, Zjawiony JK. Synthesis and evaluation of aplysinopsin analogs as inhibitors of human monoamine oxidase A and B. Bioorg Med Chem Lett. 2012;22(15):4926-4929. https://doi.org/10.1016/j.bmcl.2012.06.058

15. Huang C, Xiong J, Guan H-D, Wang C-H, Lei X, Hu JF. Discovery, synthesis, biological evaluation and molecular docking study of (R)-5-methylmellein and its analogs as selective monoamine oxidase A inhibitors. Bioorg Med Chem. 2019;27(10):2027-2040. https://doi.org/10.1016/j.bmc.2019.03.060

16. Qhobosheane MA, Petzer A, Petzer JP, Legoabe LJ. Synthesis and evaluation of 2-substituted 4 (3H)-quinazolinone thioether derivatives as monoamine oxidase inhibitors. Bioorg Med Chem. 2018;26(20):5531-5537. https://doi.org/10.1016/j.bmc.2018.09.032

17. Nel MS, Petzer A, Petzer JP, Legoabe LJ. 2-Benzylidene-1-indanone derivatives as inhibitors of monoamine oxidase. Bioorg Med Chem Lett. 2016;26(19):4599-4605. https://doi.org/10.1016/j.bmcl.2016.08.067

18. Evranos-Aksöz B, Yabanoğlu-Çiftçi S, Uçar G, Yelekçi K, Ertan R. Synthesis of some novel hydrazone and 2-pyrazoline derivatives: Monoamine oxidase inhibitory activities and docking studies. Bioorg Med Chem Lett. 2014;24(15):3278-3284. https://doi.org/10.1016/j.bmcl.2014.06.015

19. Sağlık BN, Osmaniye D, Acar Çevik U, et al. Synthesis, in vitro enzyme activity and molecular docking studies of new benzylamine-sulfonamide derivatives as selective MAO-B inhibitors. J Enzyme Inhib Med Chem. 2020;35(1):1422-1432. https://doi.org/10.1080/14756366.2020.1784892

20. Can ÖD, Osmaniye D, Demir Özkay Ü, et al. MAO enzymes inhibitory activity of new benzimidazole derivatives including hydrazone and propargyl side chains. Eur J Med Chem. 2017;131:92-106. https://doi.org/10.1016/j.ejmech.2017.03.009

21. Can NÖ, Osmaniye D, Levent S, et al. Design, synthesis and biological assessment of new thiazolylhydrazine derivatives as selective and reversible hMAO-A inhibitors. Eur J Med Chem. 2018;144:68-81. https://doi.org/10.1016/j.ejmech.2017.12.013

22. Ilgın S, Osmaniye D, Levent S, et al. Design and Synthesis of New Benzothiazole Compounds as Selective hMAO-B Inhibitors. Molecules. 2017;22(12):2187. https://doi.org/10.3390/molecules22122187

23. Can NÖ, Osmaniye D, Levent S, et al. Synthesis of New Hydrazone Derivatives for MAO Enzymes Inhibitory Activity. Molecules. 2017;22(8):1381. https://doi.org/10.3390/molecules22081381

24. Tok F, Uğraş Z, Sağlık BN, Özkay Y, Kaplancıklı ZA, Koçyiğit-Kaymakçıoğlu B. Novel 2,5-disubstituted-1,3,4-oxadiazole derivatives as MAO-B inhibitors: Synthesis, biological evaluation and molecular modeling studies. Bioorg Chem. 2021;112:104917. https://doi.org/10.1016/j.bioorg.2021.104917

25. Tok F, Sağlık BN, Özkay Y, Ilgın S, Kaplancıklı ZA, Koçyiğit-Kaymakçıoğlu B. Synthesis of new hydrazone derivatives and evaluation of their monoamine oxidase inhibitory activity. Bioorg Chem. 2021;114:105038. https://doi.org/10.1016/j.bioorg.2021.105038

ANADOLU UNIVERSITY
INSTITUTE OF HEALTH SCIENCES

European Journal of Life Sciences 2022; 1: 8-19

Research Article

Synthesis and *in silico* evaluation of some new 2,4-disubstituted thiazole derivatives

Leyla Yurttaş[1], Asaf Evrim Evren[1,2], Yusuf Özkay[1]

[1]Anadolu University, Faculty of Pharmacy, Department of Pharmaceutical Chemistry, Eskişehir, Turkey.
[2]Bilecik Şeyh Edebali University, Pharmacy Services, Vocational School of Health Services, Bilecik, Turkey.

✉ Leyla Yurttaş
lyurttas@anadolu.edu.tr

https://doi.org/10.55971/EJLS.1089425

Received: 03.17.2022
Accepted: 04.19.2022
Available online: 06.06.2022

ABSTRACT

The synthesis and antiproliferative activity investigation of methyl 3/4-[[4-(2-substituted thiazol-4-yl)phenyl]amino]-3-oxopropanoate/(4-oxobutanoate) (**3a-h**) derivatives were aimed in this work. The synthesis of the new compounds was carried out by a simple, multiple-step synthetic procedure. The physicochemical properties of the compounds were determined using SwissADME and QikProp software systems. Additionally, virtual target and toxicity predictions were carried out for all final compounds. The pharmacokinetics/physicochemical, druglikeness properties and biological target and toxicity predicitions of the compounds were determined to possess satisfying findings. Since the target determination of the compounds according to literature is point out their cytotoxic properties, the DNA gyrase enzyme was chosen as common enzymatic pathway, and evaluated via docking studies. Compound **3b**, namely methyl 4-[[4-(2-methylthiazol-4-yl)phenyl] amino]-4-oxobutanoate was detected to possess a potential to inhibit DNA gyrase-ATPase activity.

Keywords: DNA gyrase inhibition, druglikeness, molecular docking, pharmacokinetic properties, thiazole

1. INTRODUCTION

The thiazole ring is an aromatic heterocyclic ring commonly found in natural and synthetic molecules. It is existing in the structure of alkaloids, steroids, vitamins (Thiamine-vit B1), flavones, pigments and secondary metabolites [1-3]. Secondary metabolites are organic intermediates and products produced by bacteria, fungi, or plants metabolism which of those constitute important drugs in treatment [4]. Thiazole including seconder metabolites are quite large scale that some of them are penicillins, epothilones, ascidians, tubulysins, cystothiazoles, scleritodermin, leinamycin, lyngbyabellin thiostrepton and micrococcin P1 known with various biological activity potential [5].

In 1887, Hantzsch and Weber described thiazole ring, synthesis and properties [6]. In this method, known today as the Hanzsch method, α-haloketones and thioamides are reacted to form thiazoles [7]. In later years, Prop and coworkers synthesized new thiazole derivatives, in particular 2- aminothiazoles. Gabriel acquired various thiazoles by using a different implementation of Robinson-Gabriel oxazole synthesis. Tcherina obtained thiazole derivatives by cyclization reaction of α-thiocyanoketones whereas Erlenmeyer used the reaction of mercaptoketons and nitrilles. Lastly, Cook and Heilborn were developed synthetic method via α-aminonitriles, α-aminoamides and carbon disulfide. In following years, thiazole synthesis was carried out using these methods and continued in this context [8,9]. In this direction, the

synthetic suitability of the thiazole ring leads to new applications in industrial and medicinal chemistry [10]. Mono/di/polysubstituted aromatic/nonaromatic and condensed thiazoles were widely studied and it was observed that the variety of biological activities increased with changes in substitution [3,11,12].

Thiazole derivatives were reported with a broad range of biological activities such as antifungal, antibacterial, antiviral, analgesic, anticancer, anticholinesterase, antihypertensive, and antiproliferative [13-17]. Besides, in present day, thiazole core is existing in many clinically used drugs; abafungin and ravuconazole (antifungal), ritonavir (anti-HIV), febuxostat (antigut), nizatidine (antiulcer), imidacloprid (insecticide), myxothiazols and melithiazols (fungicide), fatostatin (sterol regulatory element-binding proteins (SREBPs) inhibitor), tiazofurin, bleomycin and dasatinib (anticancer), fanetizole, meloxicam and fentiazac (anti-inflammatory) sulfathiazole (antimicrobial), and nitazoxanide (antiparasitic agent) and penicillin (antibiotic) [18-20].

According to previous studies, DNA gyrase inhibition by thiazole derivatives was investigated and obtained remarkable enzyme inhibition results, even against drug-resistance pathogens [21-23]. The action mechanism of the DNA gyrase enzyme is need ATP energy. The role of the gyrase subunit B (GyrB) is to provide the energy necessary for the DNA ligation process through ATP hydrolysis, hence, the inhibition of this subunit cause stopping ATP hydrolysis, so bacteria cells lose their functions. According to literature, thiazole ring is generally linked to GyrB subunit [24,25]. Therefore, we determined the GyrB as a target.

Furthermore, in many of our studies, we conducted biological activity studies on similar [26-28] and different thiazole derivatives [29,30]. Likewise, we synthesized eight novel thiazole derivatives and evaluated their *in silico* physicochemical properties and evaluated their anti-DNA-gyrase activity, in this study.

2. MATERIALS AND METHODS

2.1. Chemistry

All chemicals were purchased from Sigma-Aldrich Chemical Co., (Sigma-Aldrich Corp., St. Louis, MO, USA) and Merck (Merck, Darmstadt, Germany). All melting points (m.p.) were determined by Electrothermal 9300 digital melting point apparatus (Electrothermal, Essex, UK) and are uncorrected. All the reactions were monitored by thin-layer chromatography (TLC) using Silica gel 60 F254 TLC plates (Merck, Darmstadt, Germany). Spectroscopic data were recorded with the following instruments: IR, Shimadzu 8400S spectrophotometer (Shimadzu, Tokyo, Japan); ^{1}H-NMR, Bruker 500 MHz spectrometer (Bruker Bioscience, Billerica, MA, USA); ^{13}C-NMR, Bruker 100 FT spectrometer (Bruker Bioscience, Billerica, MA, USA); MS, MS-FAB, VG Quattro Mass spectrometer (Fisons Instruments GmbH, Mainz, Germany) and elemental analyses were performed on a Perkin Elmer EAL 240 elemental analyser (Perkin Elmer, Norwalk, CT, USA).

2.1.1. General procedure for the synthesis of methyl 3/4-[[4-(2-substituted thiazol-4-yl)phenyl]amino]-3-oxopropanoate/(4-oxobutanoate) derivatives (3a-h)

4-(2-Substituted-4-thiazolyl)aniline derivatives (0.05 mol) **(2a-d)** were solved in tetrahydrofuran (75 mL) and triethylamine (0.06 mol). Methyl malonyl chloride/methyl succinyl chloride (0.06 mol) was added dropwise over 15 min to a magnetically stirred solution at 0-5^{o}C. After the reaction was completed, the solvent was evaporated under reduced pressure, the residue was reacted with water and filtered. The obtained resulting solid was crystallized from ethanol after dryness to gain pure final products.

Methyl 3-[[4-(2-methylthiazol-4-yl)phenyl]amino]-3-oxopropanoate **(3a)**

80-82 % yield; mp 175-179 ^{o}C. ^{1}H NMR (500 MHz, DMSO-d_6) δ 2.76 (s, 3H, CH_3), 3.49 (s, 2H, CH_2),

3.66 (s, 3H, OCH_3), 7.63 (d, 2H, *J*=8.5 Hz, Ar-H), 7.81 (s, 1H, thiazole C_5-H), 7.88 (d, 2H, *J*=8.5 Hz, Ar-H), 10.29 (s, 1H, N-H). ^{13}C NMR (125 MHz, DMSO-d_6) δ 19.39, 43.97, 53.45, 113.07, 119.66, 126.93, 130.09, 138.91, 153.98, 164.48, 165.87, 168.57. For $C_{14}H_{14}N_2O_3S$ calculated: 57.92 % C, 4.86 % H, 9.65 % N; found: 57.81 % C, 4.94 % H, 9.55 % N. MS $[M+1]^+$: *m/z* 291.

Methyl 4-[[4-(2-methylthiazol-4-yl)phenyl]amino]-4-oxobutanoate **(3b)**

76-80 % yield; mp 162-165 °C. ^{1}H NMR (500 MHz, DMSO-d_6) δ 2.61-2.65 (m, 4H, CH_2), 2.70 (s, 3H, CH_3), 3.37 (s, 3H, OCH_3), 7.63 (d, *J*=8.5 Hz, 2H, Ar-H), 7.78 (s, 1H, thiazole C_5-H), 7.85 (d, 2H, *J*=8.5 Hz, Ar-H), 10.09 (s, 1H, N-H). For $C_{15}H_{16}N_2O_3S$ calculated: 59.19 % C, 5.30 % H, 9.20 % N; found: 59.11 % C, 5.15 % H, 9.35 % N. MS $[M+1]^+$: *m/z* 305.

Methyl 3-[[4-(2-phenylthiazol-4-yl)phenyl]amino]-3-oxopropanoate **(3c)**

76-78 % yield; mp 147-150 °C. ^{1}H NMR (500 MHz, DMSO-d_6) δ 3.51 (s, 2H, CH_2), 3.67 (s, 3H, OCH_3), 7.51-7.56 (m, 3H, Ar-H), 7.69 (d, 2H, *J*=8.5 Hz, Ar-H), 7.99-8.03 (m, 5H, Ar-H), 8.08 (s, 1H, thiazole C_5-H), 10.36 (s, 1H, N-H). For $C_{19}H_{16}N_2O_3S$ calculated: 64.76 % C, 4.85 % H, 7.95 % N; found: 64.61 % C, 4.96 % H, 7.85 % N. MS $[M+1]^+$: *m/z* 353.

Methyl 4-[[4-(2-phenylthiazol-4-yl)phenyl]amino]-4-oxobutanoate **(3d)**

71-74 % yield; mp 203-206 °C. ^{1}H NMR (500 MHz, DMSO-d_6) δ 2.62-2.64 (m, 4H, CH_2), 3.61 (s, 3H, OCH_3), 7.51-7.54 (m, 3H, Ar-H), 7.69 (d, 2H, *J*=8.5 Hz), 7.98 (d, 2H, *J*=8.5 Hz, Ar-H), 8.02 (d, 2H, *J*=8.5 Hz, Ar-H), 8.06 (s, 1H, thiazole C_5-H), 10.14 (s, 1H, N-H). ^{13}C NMR (125 MHz, DMSO-d_6) δ 28.92, 31.36, 51.85, 113.77, 119.49, 126.66, 127.08, 129.31, 129.74, 130.81, 133.53, 139.71, 155.51, 167.27, 170.38, 173.34. For $C_{20}H_{18}N_2O_3S$ calculated: 65.55 % C, 4.95 % H, 7.64 % N; found: 65.64 % C, 4.99 % H, 7.75 % N. MS $[M+1]^+$: *m/z* 367.

Methyl 3-[[4-(2-(4-methoxyphenyl)thiazol-4-yl) phenyl]amino]-3-oxopropanoate **(3e)**

65-68 % yield; mp 153-158 °C. ^{1}H NMR (500 MHz, DMSO-d_6) δ 3.51 (s, 2H, CH_2), 3.67 (s, 3H, OCH_3), 3.84 (s, 3H, OCH_3), 7.08 (d, 2H, *J*=9 Hz, Ar-H), 7.67 (d, 2H, *J*=9.0 Hz, Ar-H), 7.95-8.0 (m, 5H, Ar-H), 10.34 (s, 1H, N-H). For $C_{20}H_{18}N_2O_4S$ calculated: 62.81 % C, 4.74 % H, 7.33 % N; found: 62.88 % C, 4.82 % H, 7.36 % N. MS $[M+1]^+$: *m/z* 383.

Methyl 4-[[4-(2-(4-methoxyphenyl)thiazol-4-yl)phenyl] amino]-4-oxobutanoate **(3f)**

71-74 % yield; mp 203-206 °C. ^{1}H NMR (500 MHz, DMSO-d_6) δ 2.61-2.65 (m, 4H, CH_2), 3.61 (s, 3H, OCH_3), 3.84 (s, 3H, OCH_3), 7.08 (d, 2H, *J*=8.5 Hz, Ar-H), 7.66 (d, 2H, *J*=8.5 Hz, Ar-H), 7.94-7.97 (m, 5H, Ar-H), 10.12 (s, 1H, N-H). ^{13}C NMR (125 MHz, DMSO-d_6) δ 43.51, 52.03, 55.40, 112.54, 114.64, 119.23, 125.98, 126.54, 127.43, 129.52, 138.71, 154.62, 160.90, 164.11, 166.87, 168.12. For $C_{21}H_{20}N_2O_4S$ calculated: 63.62 % C, 5.08 % H, 7.07 % N; found: 63.66 % C, 4.98 % H, 7.15 % N. MS $[M+1]^+$: *m/z* 397.

Methyl 3-[[4-(2-(4-fluorophenyl)thiazol-4-yl)phenyl] amino]-3-oxopropanoate **(3g)**

63-68 % yield; mp 184-186 °C. ^{1}H NMR (500 MHz, DMSO-d_6) δ 3.67 (s, 2H, CH_2), 3.83 (s, 3H, OCH_3), 7.37 (brs, 2H, Ar-H), 7.69 (brs, 2H, Ar-H), 7.99-8.21 (m, 5H, Ar-H), 10.33 (s, 1H, N-H). For $C_{19}H_{15}FN_2O_3S$ calculated: 61.61 % C, 4.08 % H, 7.56 % N; found: 61.69 % C, 4.19 % H, 7.65 % N. MS $[M+1]^+$: *m/z* 370.

Methyl 4-[[4-(2-(4-fluorophenyl)thiazol-4-yl)phenyl] amino]-4-oxobutanoate **(3h)**

65-69 % yield; mp 200-203 °C. ^{1}H NMR (500 MHz, DMSO-d_6) δ 2.62-2.64 (m, 4H, CH_2), 3.80 (s, 3H, OCH_3), 7.38 (brs, 2H, Ar-H), 7.72 (brs, 2H, Ar-H), 7.98-8.20 (m, 5H, Ar-H), 10.35 (s, 1H, N-H). ^{13}C NMR (125 MHz, DMSO-d_6) δ 28.42, 30.93, 51.42, 113.34, 116.25, 116.38, 126.68, 128.42,

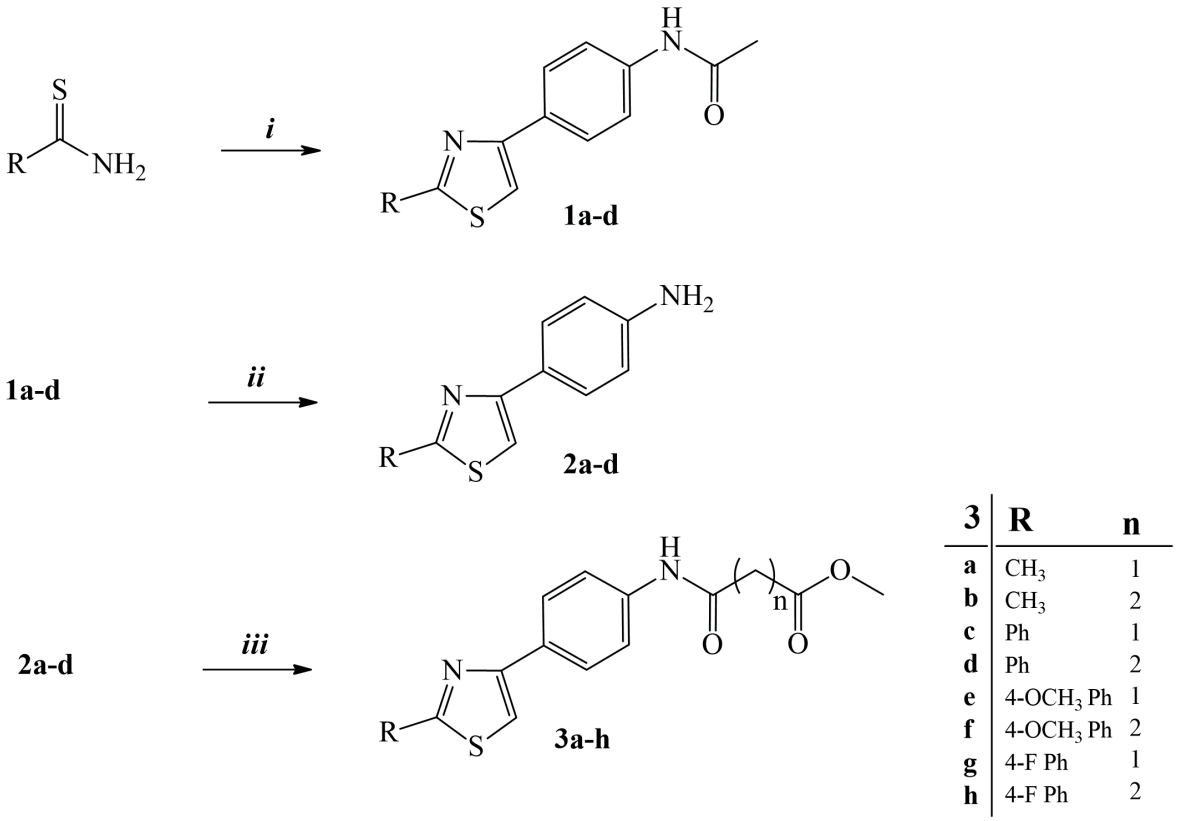

3	R	n
a	CH_3	1
b	CH_3	2
c	Ph	1
d	Ph	2
e	4-OCH_3 Ph	1
f	4-OCH_3 Ph	2
g	4-F Ph	1
h	4-F Ph	2

Scheme 1. The synthetic protocol of the compounds **3a-h.** Reactants and conditions: : ***i*** : 4-(2-bromoacetyl)acetanilide, EtOH, r.t., 8h; ***ii*** : 10 % HCl , EtOH, reflux; ***iii*** : methyl malonyl chloride/methyl succinyl chloride, TEA, THF, r.t.

125.53, 128.79, 129.76, 139.25, 155.0, 162.25, 164.23, 165.65, 169.80, 172.83. For $C_{20}H_{17}FN_2O_3S$ calculated: 62.49 % C, 4.46 % H, 7.29 % N; found: 62.59 % C, 4.35 % H, 7.25 % N. MS $[M+1]^+$: *m/z* 384.

2.2. *In Silico* Prediction

The physicochemical properties of the compounds were calculated using SwissADME [31] and Qikprop [32] software programs. Potential activity and toxicity profiles were predicted using SwissTargetPrediction [33] and pkCSM–pharmacokinetics [34] software programs. The DNA-gyrase crystal was retrieved from RCSB Protein Data Bank (PDBID: 4DUH), and the protein and final compounds prepared using protein preparation and ligand preparation wizards at 7.4±1.0 pH. Their binding modes were investigated using Maestro software program.

3. RESULTS AND DISCUSSION

Present study was undertaken to synthesize methyl 3/4-[[4-(2-substituted thiazol-4-yl)phenyl] amino]-3-oxopropanoate/(4-oxobutanoate) (**3a-h**) derivatives and to evaluate their *in silico* physicochemical properties. The synthetic protocol was realized according to previously reported studies [26] and it was depicted in **Scheme 1**. Initially, thiazole derivatives were synthesized according to Hantzsch thiazole synthesis with the reaction of alkyl/aryl thioamides and α-bromo-(4'-acetylamino)acetophenone. Then the obtained thiazole intermediates (**1a-d**) were hydrolyzed to convert acetanilide to corresponding aniline. Lastly, the acquired 4-(2-substituted-4-thiazolyl)aniline derivatives (**2a-d**) were reacted with methyl malonyl chloride or methyl succinyl chloride at acetylation conditions to reach ester compounds (**3a-h**). The

Table 1. Some properties of synthesized compounds from SwissADME

	HBA	HBD	TPSA	Log $P_{o/w}$	SC	Log K_p	GIA	RoF (V)	Ghose	Leadlikeness (V)
3a	4	1	96.53	2.38	Moderately	6.11	High	0	Yes	Yes
3b	4	1	96.53	2.48	Moderately	6.77	High	0	Yes	Yes
3c	4	1	96.53	3.50	Poorly	5.59	High	0	Yes	No (2)
3d	4	1	96.53	3.62	Poorly	6.26	High	0	Yes	No (2)
3e	5	1	105.76	3.48	Poorly	5.79	High	0	Yes	No (3)
3f	5	1	105.76	3.60	Poorly	6.46	High	0	Yes	No (2)
3g	5	1	96.53	3.77	Poorly	5.63	High	0	Yes	No (2)
3h	5	1	96.53	3.93	Poorly	6.29	High	0	Yes	No (2)

MW: Molecular Weight, **HBA:** H-bond acceptor, **HBD:** H-bond acceptor, **TPSA:** Topologic polar surface area (Å²) **Log $P_{o/w}$:** *Consensus* Log $P_{o/w}$ (Average of all five predictions), **SC:** Solubility Class (Water), **GIA:** Gastrointestinal absorption, **Log K_p:** skin permeation **(-cm/s)**, **RoF (V)**: Rule of Five (violation number), **Ghose:** Ghose Filter, **Leadlikeness (V):** Suitability score (violation number).

Table 2. Some properties of synthesized compounds from Schrodinger (QikProp)

	HBA	HBD	PSA	Log $P_{o/w}$	AS	-Log K_p	%HOA	RoF (V)	RoT (V)	Similar Molecules
3a	5	0	81.10	2.74	-4.20	-2.56	96	0	0	Azapropazone
3b	6	1	82.09	2.75	-4.76	-2.53	96	0	0	Diloxanide
3c	5	0	79.52	4.08	-5.80	-1.83	100	0	1	Phenylbutazone
3d	6	1	80.51	3.98	-6.20	-1.80	100	0	1	Oxyphenbutazone
3e	5.75	0	88.0	4.09	-5.84	-1.94	100	0	1	Bisacodyl
3f	6.75	1	88.99	4.09	-6.35	-1.91	100	0	1	Famprofazone
3g	6	1	80.51	4.28	-6.60	-1.94	100	0	1	Bisacodyl
3h	5	0	79.5	4.32	-6.17	-1.96	100	0	1	Tribuzone

HBA: H-bond acceptor (2 / 20), **HBD:** H-bond acceptor (0 / 6), **PSA:** vdW Polar SA (7.0 / 200.0), **%HOA:** % Human Oral Absorption in GI (poor<%25), **Log $P_{o/w}$:** Log $P_{o/w}$ (-6.5 / 0.5), **AS:** log S for aqueous solubility (-6.5 / 0.5), **Log K_p:** skin permeability **(cm/hr)**, **RoF (V)**: Rule of Five (violation number), **RoT (V):** Jorgensen Rule of 3 Violations, **Similar Molecules:** At least 90% similarity and above were considered, but if there is nothing, at this time the closest one indicated.

structure of final compounds was assigned on the basis of spectroscopic and analytical data. In the ^{1}H-NMR spectra of the compounds, singlet peaks at about 3.37-3.83, 7.78-8.08 and 10.09-10.36 ppm were assigned to methoxy proton (OCH_3), thiazole C_5 proton and NH protons, respectively. The other alkylic and aromatic protons were determined at about 2.61-3.51 ppm and 7.08-8.21 ppm. In the ^{13}C-NMR spectra of the compounds, peaks at about 51.85-53.45 ppm indicated the methoxy carbon existed in ester structure, the signals observed in the down field over 160 ppm were defined for carbonyl carbons and vicinal aromatic carbons to heteroatoms as expected. M+1 peaks were determined for all compounds. Elemental analyses results for C, H, and N elements were satisfactory within calculated values of the compounds.

The physicochemical/pharmacokinetic and druglikeness properties of the final compounds (**3a-h**) were predicted using SwissADME (**Table 1**) and QikProp (**Table 2**) softwares. ADME parameters (for Absorption, Distribution, Metabolism and Excretion) including H-bond acceptor (HBA), H-bond acceptor (HBD), polar surface area (PSA/TPSA), partition coefficient (Log Po/w), skin permeability (Log Kp), Rule of five (violation number-RoF) and Gastrointestinal absorption (GIA) were calculated virtually in both programs. Additionally, water solubility (Log S), Jorgensen Rule of 3 Violations (RoT(V), Molecular Weight (MW) were identified and evaluated [35]. According to the Lipinski Rule of Five, all compounds were detected in the compliant with the rule to be an oral bioavailable drug. The rule suggests that a high absorption is available for an

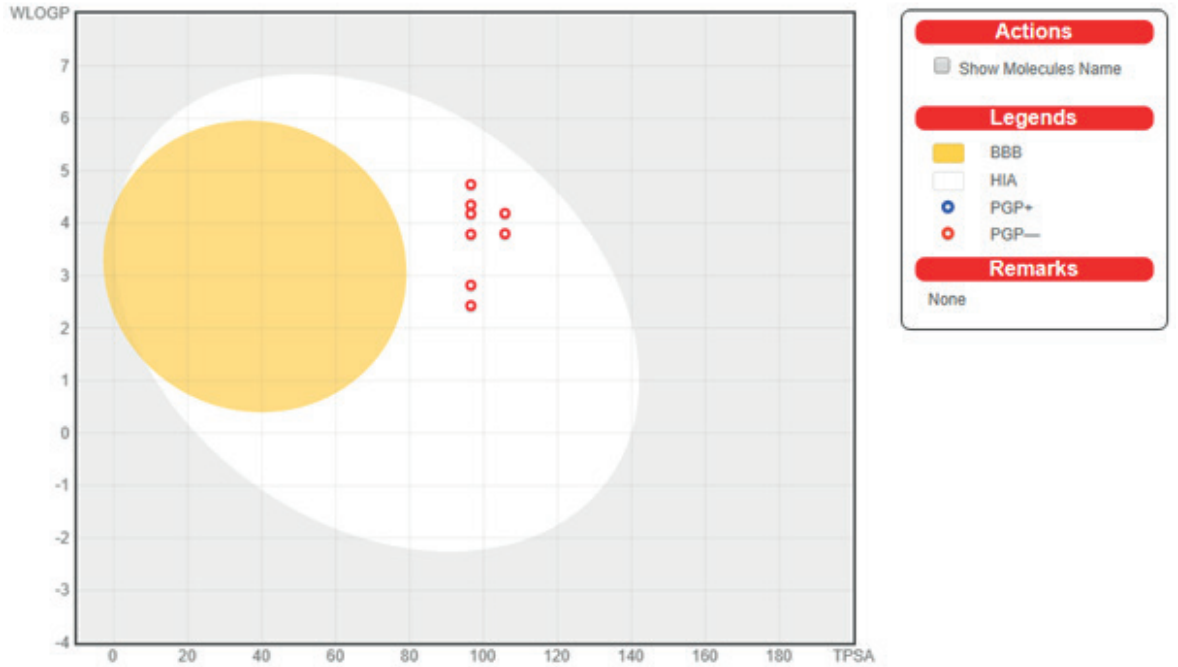

Figure 1. Boiled-egg plot of the compounds **3a-h**

oral drug when it possesses HBD less than 5, HBA less than 10, MW less than 500, and log P less than 5 [36]. All compounds passed Ghose filter developed by him [37] for drug discovery. Leadlikeness is the filter identified by Teague and co-workers which only compounds **3a** and **3b** passed through this filter [38]. Also, similar molecules (anti-inflammatory, antiprotozoal and laxative drugs) to these compounds were detected by QikProp software The boiled-egg plot between WLOGP and TPSA was also studied in SwissADME to predict gastrointestinal absorption and brain penetration of the selected molecules. According to **Figure 1**, none of the compounds have BBB permeability but they possess gastrointestinal absorption. Besides, red dots show molecules predicted not to be effluated from central nervous system by P-glycoprotein [39].

Table 3. SwissTarget prediction of the compounds **3a-h** in percentage (%)

	Kinase	Enzyme	Family A G protein-coupled receptor
3a	33.3	13.3	13.3
3b	26.7	13.3	13.3
3c	60	-	-
3d	53.3	-	13.3
3e	40	-	13.3
3f	40	20	-
3g	53.3	13.3	-
3h	33.3	20	20

Target prediction of the final compounds was identified using SwissTarget prediction software. Top fifteen targets were estimated; frequently predicted target regions were given in **Table 3** and over 10 % were in explanation. Compounds **3a-h** were determined to target on kinase, enzyme and Family A G protein-coupled receptor with percentages of 26.7-60, 13.3-20 and 13.3-20 %, respectively. Additionally, compound **3a** and **3c** exhibited phosphodiesterase target with 13.3 and 26.7 %. Compound 3b showed Family B G protein-coupled receptor (13.3%) whereas **3d** showed nuclear receptor (26.7%). Besides, compound **3e**, **3f** and **3g** represented targets phosphatase, electrochemical

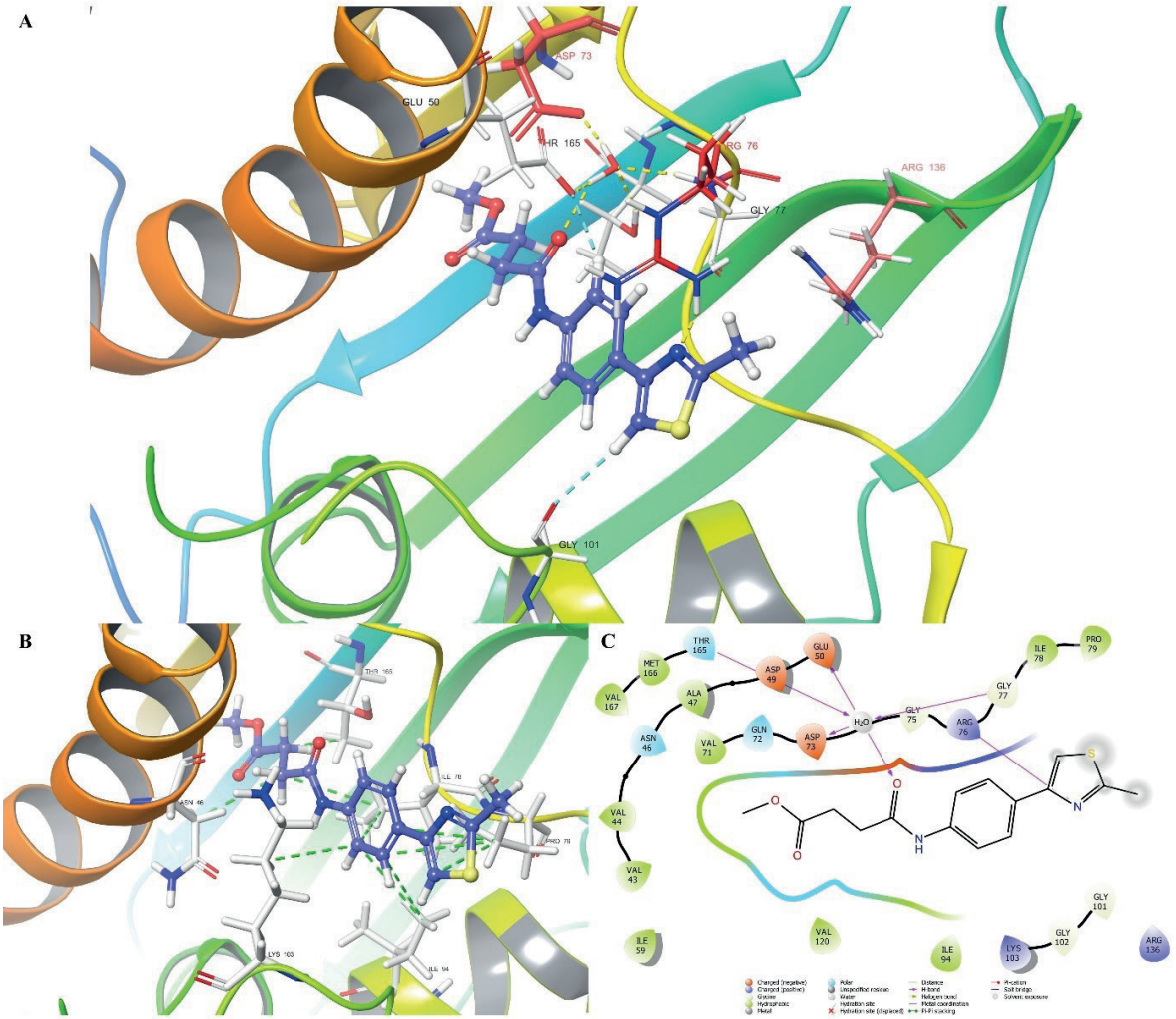

Figure 2. The best 2D and 3D poses of compound **3b. A)** The carbon atoms of key amino acids were represented as red, the carbon atoms interacted residues were represented as white. **B)** Hydrophobic interactions were represented as green dashes. **C)** The ligand, the residues around its 5 Å, and the important water molecule were displayed.

transporter and protease with percentages 13.3, 13.3 and 20 %, respectively. The possible sites of target which the compound may bind to are mostly the targets which are predicted by the software and the probability score are very less that is between 0.153 to 0.097. This makes an inference that the small compound may have high target attraction towards the specific binding site it is directed to [40].

In addition to the above information, we investigated the probable antimicrobial action mechanism of the final compounds through the docking study. The docking study point out that compound **3b** may have potent antimicrobial activity via ATP-competitive DNA gyrase B inhibition. Obtained 2D and 3D pose showed that compound **3b** interacted with Asp49, Glu50, Asp73 and Gly77 amino acids via water-mediated H-bonds. On the other hand, there were one direct H-bond with Arg76 and also 2 aromatic H-bonds with Gly101 and Thr165 residues. Moreover, compound **3b** have showed van der Waals

interactions with Asn46, Ile78, Pro79, Ile94, Lys103 and Thr165 amino acids. All those connections were envisaged as binding action (**Figure 2**). The role of the GyrB subunit is to provide the energy necessary for the DNA ligation process through ATP hydrolysis, hence, the inhibition of this subunit cause stopping ATP hydrolysis, so bacteria cells lose their functions. In previous studies, Asp73 and Gly101 residues have been described as key amino acids for inhibition of the GyrB subunit [41,42]. However, Gly101 amino acid and the other loop amino acids (Gly102, Lys103, and Phe104) could stabilize the loop region, which reduces the flexibility of the enzyme. Therefore, it can be concluded that be a direct proportion between the strong inhibition potential and those loop amino acids interactions. Moreover, final compounds except **3b**, could not properly enter the cavity, thus, not dock with important amino acids well at GyrB active pocket (**Figure 3**). For compounds **3c-3h**, It is probably caused by their bulky structures due to phenyl substitutions at the 4th position of the thiazole ring. On the other hand, compound **3a** has a small moiety (methyl) at thiazole ring like **3b**, but its localization was observed like other derivatives. It may be related to the absence of one carbon at the side chain. This absence may have led to unfavorable localization between ligand and protein. Indeed, there weren't any connections between **3a** and Gly101. It's clear that only compound **3b** was found as an appropriate analog to inhibit DNA gyrase via blocking ATP hydrolysis. In further studies, the advanced experimental studies should be improved. Although this potential hit was determined, this compound may also be useful for developing more powerful molecules.

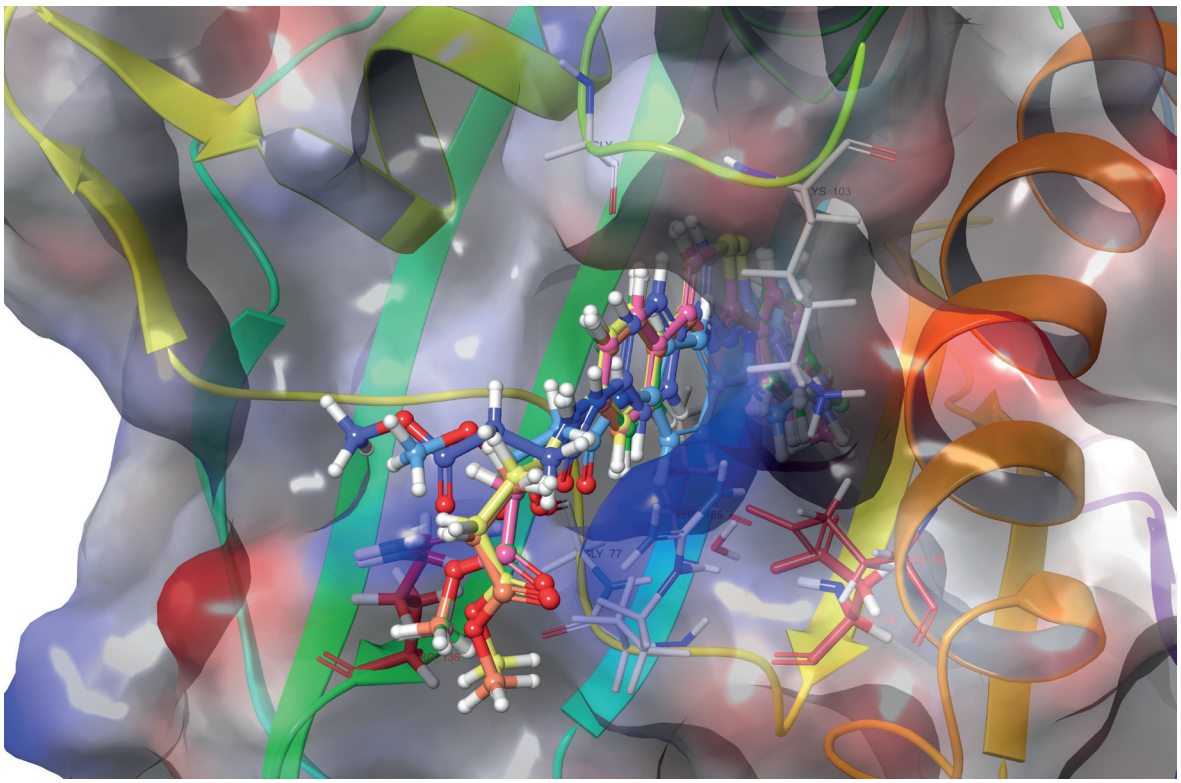

Figure 3. The final compounds at DNA gyrase active region

Table 4. Toxic profiles of the compounds (**3a-h**) predicted using pkCSM software

	3a	**3b**	**3c**	**3d**	**3e**	**3f**	**3g**	**3h**
Ames toxicity	No	No	No	No	No	No	No	No
Max. tolerated dose (human, log mg/kg/day)	-0.156	-0.198	-0.054	-0.025	-0.118	-0.107	-0.102	-0.089
hERG I inhibitor	No	No	No	No	No	No	No	No
hERG II inhibitor	No	No	No	No	No	No	No	No
Oral Rat Acute Toxicity (LD50, mol/kg)	2.686	2.643	2.243	2.147	2.447	2.37	2.38	2.304
Oral Rat Chronic Toxicity (LOAEL, log mg/kg_bw/day)	1.178	1.169	0.911	0.909	1.01	0.936	0.974	0.901
Hepatoxicity	Yes	Yes	Yes	Yes	Yes	Yes	Yes	Yes
Skin sensitisation	No	No	No	No	No	No	No	No
***T. pyriformis* toxicity (log µg/L)**	0.887	1.127	0.567	0.562	0.46	0.451	0.462	0.455
Minnow toxicity (log mM)	0.881	0.719	-0.382	-0.511	-0.837	-0.966	-0.631	-0.76

Toxic profiles of the compounds were also predicted using pkCSM software and the results were displayed in **Table 4**. The website can provide details of toxicology effects in the fields of AMES toxicity, human maximum tolerance dose, hERG-I inhibitor, hERG-II (human Ether-à-go-go-Related Gene) inhibitor, LD_{50} (lethal dose), chronic oral rat toxicity, hepatotoxicity, skin toxicity, *T. pyriformis* toxicity and minnow toxicity. None of the compounds possessed Ames toxicity which mean they have no mutagenic potential and also skin sensitization, however they all cause hepatotoxicity. They don't inhibit hERG-I and hERG-II which is a satisfying finding that provides non-cardiotoxic profile to the compounds [43]. Acute oral rat toxicity (LD_{50}) of the compounds were found in between 2.147-2.686 mol/kg, whereas chronic oral rat toxicity (LOAEL) were found 0.901-1.178 log mg/kg_bw/day. Toxicity to *T. pyriformis* which is a ciliate protozoan was found between the range of 0.451-1.127 log µg/L. Compounds **3a** and **3b** including alkyl function (methyl) which differ from others showed the highest toxicity to the protozoan and minnow (fish species), too.

4. CONCLUSION

New eight thiazole compounds (**3a-h**) were synthesized containing ester and amide function using known synthetic procedures and starting from Hantzsch thiazole ring cyclization reaction. Final ester compounds were evaluated for their physicochemical/pharmacokinetic and druglikeness properties. All compounds were found to be in compliance with such rules, Lipinski and Ghose. Kinases were *in silico* determined as the main biological target for these compounds and toxicity profile of them was identified at the acceptable ranges, virtually. Compound **3b** was found a hit molecule to inhibit DNA gyrase B subunit enzyme.

Ethical approval

Not applicable, because this article does not contain any studies with human or animal subjects.

Author contribution

Concept: LY, YÖ; Design: LY, YÖ; Supervision: YÖ; Materials: LY; Data Collection and/or Processing: LY, AEE; Analysis and/or Interpretation: LY, YÖ, AEE; Literature Search: LY, AEE; Writing: LY, AEE; Critical Reviews: LY, AEE.

Source of funding

The authors declare the study received no funding.

Conflict of interest

The authors declare that there is no conflict of interest.

REFERENCES

1. Nayak S, Gaonkar SL. A review on recent synthetic strategies and pharmacological importance of 1,3-thiazole derivatives. Mini Rev Med Chem. 2019;19:215-238. https://doi.org/10.2174/1389557518666180816112151
2. Yılmaz Cankılıç M, Yurttaş L. Study on the antimicrobial effects of novel thiazole derivatives. Marmara Pharm J. 2017;21(3):654-659. https://doi.org/10.12991/marupj.323584
3. Kashyap SJ, Vipin Kumar G, Kumar Sharma P, Kumar N, Dudhe R, Kumar Gupta J. Thiazoles: having diverse biological activities. Med Chem Res. 2012;21:2123-2132. https://doi.org/10.1007/s00044-011-9685-2
4. Bourgaud F, Gravot A, Milesi, S, Gontier E. Production of plant secondary metabolites: a historical perspective. Plant Sci. 2001;161(5):839-851. https://doi.org/10.1016/S0168-9452(01)00490-3
5. Rouf A, Tanyeli C. Bioactive thiazole and benzothiazole derivatives. Eur J Med Chem. 2015:97;911-927. https://doi.org/10.1016/j.ejmech.2014.10.058
6. Akbarzadeh A, Soleymani R, Taheri M, Karimi-Cheshmeh Ali M. Synthesis new and novel aryl thiazole derivatives compounds. Orient J Chem. 2012;28(1):153-164. http://www.orientjchem.org/?p=23776
7. Deepti V, Aruna Kumari M, Harikrishna N, Ramesh G, Venkata Rao C. Synthesis of novel 2-amino thiazole derivatives. Der Pharm Chem. 2013;5(2):181-184. https://www.derpharmachemica.com/pharma-chemica/synthesis-of-novel-2amino-thiazole-derivatives.pdf
8. Chhabriaa MT, Patel S, Modi P, Brahmkshatriya PS. Thiazole: A review on chemistry, synthesis and therapeutic importance of its derivatives. Curr Top Med Chem. 2016;16:2841-2862. https://doi.org/10.2174/1568026616666160506130731
9. Ibrahim Mohamed SS. Synthesis of new thiazole derivatives bearing a sulfonamide moiety of expected anticancer and radiosensitizing activities [master's thesis]. Cairo: Cairo University; 2012. https://inis.iaea.org/collection/NCLCollectionStore/_Public/45/099/45099941.pdf
10. Kashyap A, Adhikari N, Das A, et al. Review on synthetic chemistry and antibacterial importance of thiazole derivatives. Curr Drug Dis Techno. 2018;15:214-228. https://doi.org/10.2174/1570163814666170911144036
11. Tomassetti M, Lupidi G, Piermattei P, et al. Catalyst-free synthesis of polysubstituted 5-acylamino-1,3-thiazoles via Hantzsch cyclization of α-chloroglycinates. Molecules. 2019;24:3846. https://doi.org/10.3390/molecules24213846
12. Evren AE, Yurttas L, Ekselli B, Akalin-Ciftci G. Synthesis and biological evaluation of 5-methyl-4-phenyl thiazole derivatives as anticancer agents. Phosphorus Sulfur Silicon Relat Elem. 2020;194(8):820-828. https://doi.org/10.1080/10426507.2018.1550642
13. Sahin Z, Ertas M, Bender C, et al. Thiazole-substituted benzoylpiperazine derivatives as acetylcholinesterase inhibitors. Drug Dev Res. 2018;79(8):406-425. https://doi.org/10.1002/ddr.21481
14. Siddiqui N, Arshad MF, Ahsan W, Alam MS. Thiazoles: A valuable insight into the recent advances and biological activities. Inter J Pharma Sci Drug Res. 2009;1(3):136-143. https://ijpsdr.com/index.php/ijpsdr/article/view/46
15. Doregiraee A, Kermani ET, Khabazzadeh H, Pouramiri B. Synthesis of new 1,3-thiazole derivatives; using 1-(4-carbamoylphenyl)-3- methylthiourea and 1-methyl-3-(quinolin-8-yl)thiourea as starting materials. J Chil Chem Soc. 2015;6:3021-3023. https://doi.org/10.4067/S0717-97072015000300009
16. Gaikwad SA, Patil AA, Deshmukh MB. An efficient, uncatalyzed, and rapid synthesis of thiazoles and aminothiazoles under microwave irradiation and investigation of their biological activity. Phosphorus Sulfur Silicon Relat Elem. 2010;185:103-109. https://doi.org/10.1080/10426500802715163

17. Yurttaş L, Özkay Y, Demirci F, et al. Synthesis, anticandidal activity, and cytotoxicity of some thiazole derivatives with dithiocarbamate side chains. Turk J Chem. (2014);38:815-24 https://doi.org/10.3906/kim-1312-62

18. Maienfisch P, Edmunds AJF. Thiazole and isothiazole ringe containing compounds in crop protection. Adv Heterocyc Chem. 2010;121:35-88. https://doi.org/10.1016/bs.aihch.2016.04.010

19. Ayati A, Emami S, Asadipour A, Shafiee A, Foroumadi A. Recent applications of 1,3-thiazole core structure in the identification of new lead compounds and drug discovery. Eur J Med Chem. 2015;97:699-718. https://doi.org/10.1016/j.ejmech.2015.04.015

20. Ayati A, Emami S, Moghimi S, Foroumadi A. Thiazole in the targeted anticancer drug discovery. Future Med Chem. 2019;11(15):1929-1952. https://doi.org/10.4155/fmc-2018-0416

21. Ali Mohamed H, Ammar YA, A M Elhagali G, A Eyada H, S Aboul-Magd D, Ragab A. In Vitro Antimicrobial Evaluation, Single-Point Resistance Study, and Radiosterilization of Novel Pyrazole Incorporating Thiazol-4-one/Thiophene Derivatives as Dual DNA Gyrase and DHFR Inhibitors against MDR Pathogens. ACS Omega. 2022;7(6):4970-4990. https://doi.org/10.1021/acsomega.1c05801

22. Moussaoui O, Bhadane R, Sghyar R, et al. Design, Synthesis, in vitro and in silico Characterization of 2-Quinolone-L-alaninate-1,2,3-triazoles as Antimicrobial Agents. ChemMedChem. 2022;17(5):e202100714. https://doi.org/10.1002/cmdc.202100714

23. Yang XC, Zhang PL, Kumar KV, Li S, Geng RX, Zhou CH. Discovery of unique thiazolidinone-conjugated coumarins as novel broad spectrum antibacterial agents. Eur J Med Chem. 2022;232:114192. https://doi.org/10.1016/j.ejmech.2022.114192

24. Evren AE, Dawbaa S, Nuha D, Yavuz ŞA, Gül ÜD, Yurttaş L. Design and synthesis of new 4-methylthiazole derivatives: In vitro and in silico studies of antimicrobial activity. J Mol Struct. 2021;1241:130692. https://doi.org/10.1016/j.molstruc.2021.130692

25. Stanger FV, Dehio C, Schirmer T. Structure of the N-terminal Gyrase B fragment in complex with ADPPi reveals rigid-body motion induced by ATP hydrolysis. PLoS One. 2014;9(9):e107289. https://doi.org/10.1371/journal.pone.0107289

26. Özkay Y, Yurttaş L¸ Dikmen M, Engür S. Synthesis and antiproliferative activity evaluation of new thiazole–benzimidazole derivatives using real-time cell analysis (RTCA DP). Med Chem Res. 2016;25:482-493. https://dx.doi.org/10.1007/s00044-016-1507-0

27. Yurttaş L, Özkay Y, Akalın-Çiftçi G, Ulusoylar-Yıldırım Ş. Synthesis and anticancer activity evaluation of N-[4-(2-methylthiazol-4-yl)phenyl]acetamide derivatives containing (benz)azole moiety. J Enzyme Inhib Med Chem. 2014;29(2):175-184. https://doi.org/10.3109/14756366.2013.763253

28. Yurttaş L, Kaplancıklı ZA, Özkay Y. Design, synthesis and evaluation of new thiazole-piperazines as acetylcholinesterase inhibitors. J Enzyme Inhib Med Chem. 2013;28(5):1040-1047. https://doi.org/10.3109/14756366.2012.709242

29. Yurttaş L, Demir B, Akalın-Çiftçi G. Some thiazole derivatives combined with different heterocycles: cytotoxicity evaluation and apoptosis inducing studies. Anticancer Agents Med Chem. 2018;18:1115-1121. https://doi.org/10.2174/1871520618666180328115314

30. Demirayak Ş, Şahin Z, Ertaş M, et al. Novel thiazole-piperazine derivatives as potential cholinesterase inhibitors. J Heterocyclic Chem. 2019;56(12):3370-3386. https://doi.org/10.1002/jhet.3734

31. SwissADME. Swiss Institute of Bioinformatics. (2021). Retrieved 15 January, 2022 from http://www.swissadme.ch/

32. QikProp. Rapid ADME predictions of drug candidates. (2022). Retrieved 25 January, 2022 from https://www.schrodinger.com/qikprop

33. SwissTargetPrediction. Swiss Institute of Bioinformatics. (2021). Retrieved 20 January, 2022 from http://www.swisstargetprediction.ch/

34. pkCSM. Pharmacokinetic properties. (2021). Retrieved 10 June, 2021 from http://biosig.unimelb.edu.au/pkcsm/admet_prediction

35. Daina A, Michielin O, Zoete V. SwissADME: a free web tool to evaluate pharmacokinetics, drug-likeness and medicinal chemistry friendliness of small molecules. Sci Rep. 2017;7:42717. https://doi.org/10.1038/srep42717

36. Ertas M, Biltekin SN, Berk B, Yurttaş L, Demirayak Ş. Synthesis of some 5,6-diaryl-1,2,4-triazine derivatives and investigation of their cyclooxygenase (COX) inhibitory activity. Phosphorus Sulfur Silicon Relat Elem. Forthcoming 2022. https://doi.org/10.1080/10426507.2022.2062756

37. Ghose AK, Viswanadhan VN, Wendoloski JJ. A knowledge-based approach in designing combinatorial or medicinal chemistry libraries for drug discovery. A qualitative and quantitative characterization of known drug databases. J Comb Chem. 1999;1:55-68. https://doi.org/10.1021/cc9800071

38. Teague S, Davis A, Leeson P, Oprea T. The design of leadlike combinatorial libraries. Angew Chem Int Ed Engl. 1999:38;3743-3748. https://doi.org/10.1002/(SICI)1521-3773(19991216)38:24<3743::AID-ANIE3743>3.0.CO;2-U

39. Tukur M, Adamu I, Gideon U, Shallangwa A, Uba S. In-silico activity prediction and docking studies of some 2,9-disubstituted 8-phenylthio/phenylsulfinyl-9h-purine derivatives as anti-proliferative agents. Heliyon. 2020;6:e03158. https://doi.org/10.1016/j.heliyon.2020.e03158

40. Enmozhi SK, Raja K, Sebastine I, Joseph J. Andrographolide as a potential inhibitor of SARS-CoV-2 main protease: an in silico approach. J Biomol Struct Dyn. 2021;39(9):3092-3098. https://doi.org/10.1080/07391102.2020.1760136

41. Durcik M, Nyerges Á, Skok Ž, et al. New dual ATP-competitive inhibitors of bacterial DNA gyrase and topoisomerase IV active against ESKAPE pathogens. Eur J Med Chem. 2021;213:113200. https://doi.org/10.1016/j.ejmech.2021.113200

42. Durcik M, Lovison D, Skok Ž, et al. New N-phenylpyrrolamide DNA gyrase B inhibitors: Optimization of efficacy and antibacterial activity. Eur J Med Chem. 2018;154:117-132. https://doi.org/10.1016/j.ejmech.2018.05.011

43. Wang S, Li Y, Xu L, Li D, Hou T. Recent developments in computational prediction of HERG blockage. Curr Top Med Chem. 2013;13(11):1317-1326. https://doi.org/10.2174/15680266113139990036

ANADOLU UNIVERSITY
INSTITUTE OF HEALTH SCIENCES

European Journal of Life Sciences 2022; 1: 20-27

Research Article

Design, synthesis and *in vitro* COX inhibitory profiles of a new series of tetrazole-based hydrazones

Mehlika Dilek Altıntop[1], Belgin Sever[1], Halide Edip Temel[2], Zafer Asım Kaplancıklı[1], Ahmet Özdemir[1]

[1]Anadolu University, Faculty of Pharmacy, Department of Pharmaceutical Chemistry, Eskişehir, Turkey.
[2]Anadolu University, Faculty of Pharmacy, Department of Biochemistry, Eskişehir, Turkey.

✉ Mehlika Dilek Altıntop
mdaltintop@anadolu.edu.tr

https://doi.org/10.55971/EJLS.1095818

Received: 03.30.2022
Accepted: 04.20.2022
Available online: 06.06.2022

ABSTRACT

Inhibition of cyclooxygenases (COXs) by selective and nonselective inhibitors is a favorable approach for pharmacologic intervention in a variety of disorders such as cancer. For this purpose, a new class of tetrazole-hydrazone hybrids (**1-12**) was designed. A facile and efficient three-step procedure was applied for the preparation of compounds **1-12**, which were tested for their inhibitory activities towards cyclooxygenases (COXs) by means of an *in vitro* colorimetric inhibitor screening method. The most potent and selective COX-1 inhibitors were determined as 2-[(1-methyl-1*H*-tetrazol-5-yl)thio]-*N*'-(4-(piperidin-1-yl)benzylidene) acetohydrazide (**1**) (40.88±2.79%) and 2-[(1-methyl-1*H*-tetrazol-5-yl)thio]-*N*'-(4-(morpholin-4-yl)benzylidene)acetohydrazide (**2**) (39.80±2.78%), whereas the most potent and selective COX-2 inhibitor was found as 2-[(1-phenyl-1*H*-tetrazol-5-yl)thio]-*N*'-(4-(pyrrolidin-1-yl) benzylidene)acetohydrazide (**10**) (42.38±1.16%). In general, 1-methyl-1*H*-tetrazole moiety resulted in selective COX-1 inhibition, whereas 1-phenyl-1*H*-tetrazole moiety gave rise to preferential COX-2 inhibition.

Keywords: Cyclooxygenase, hydrazone, synthesis, tetrazole

1. INTRODUCTION

Prostaglandins (PGs) and thromboxane A_2 (TXA_2) belong to a class of lipid signaling molecules derived from arachidonic acid (AA) [1]. Biosynthesis of PGs and TXA_2 is catalyzed by two cyclooxygenase (COX) isoforms, COX-1 and COX-2 [1,2], which have similar structural and catalytic properties [3]. However, both enzymes differ in terms of their regulation of expression, tissue distribution, and pharmacological functions [3,4]. COX-1 is constitutively expressed in many tissues (e.g., thrombocytes, gastrointestinal tract, lung, kidney, liver, brain, spleen and prostate), where COX-1-derived prostanoids participate in homeostatic functions. Under normal physiological conditions, COX-1-derived prostanoids play a fundamental role in the maintenance of platelet function, renal perfusion, and cytoprotective levels of PGs in the gastric mucosa [3-6]. On the contrary, COX-2 is frequently referred to as the inducible isoform, responsible for enhanced PG production in response to inflammatory and mitogenic stimuli [4-7]. The up-regulation and overexpression of COX-2 lead to inflammation, loss of apoptosis, uncontrolled cell proliferation, metastasis, and angiogenesis finally resulting in cancer [8].

Today, the concept of "constitutive" and "inducible" isoforms has been challenged [4] by mounting evidence pointing out that COX-2 is also constitutively expressed in some tissues [9]

and COX-1 is up-regulated in various pathological conditions including thrombosis, atherosclerosis, and tumorigenesis [10].

Inhibition of COXs by a variety of selective and nonselective inhibitors is a promising approach for pharmacologic intervention in many pathological conditions [11,12].

Hydrazides-hydrazones are not only useful intermediates for the synthesis of various heterocyclic compounds but also frequently occurring motifs in drug molecules [13-16] due to their diverse pharmacological activities such as anti-inflammatory, analgesic, antidepressant, anticonvulsant, antitumor, antimycobacterial, and antimalarial activities [13-21]. In particular, the anti-inflammatory potency of hydrazones is well-documented and some of them exert their action through the inhibition of COXs [17-21].

Tetrazole scaffold is reported to be among the top 25 most commonly utilized nitrogen heterocycles in pharmaceutical agents [22]. The tetrazole ring is a well-known bioisostere of the carboxylic acid group [23] and therefore this core is frequently used for the design of promising COX inhibitors for the management of inflammation [24,25].

Prompted by aforementioned data [17-25], the facile and efficient synthesis of a novel series of tetrazole-based hydrazones (**1-12**) was performed and *in vitro* studies were conducted to assess their inhibitory effects on COXs.

2. MATERIALS AND METHODS

2.1. Chemicals and Equipments

All chemicals were purchased from commercial suppliers and were used without further purification. The melting points (M.p.) of the compounds were detected on a MP90 digital melting point apparatus (Mettler Toledo, Ohio, USA) and are uncorrected. Rotavapor® R-100 (Büchi, Switzerland) was used for the evaporation of the solvents. Nuclear Magnetic Resonance (NMR, ^{1}H and ^{13}C) spectra were recorded on a Bruker spectrometer (Bruker, Billerica, MA, USA). Chemical shifts were reported in parts per million (ppm) and the coupling constants (*J*) were expressed in Hertz (Hz). and High Resolution Mass Spectrometry (HRMS) spectra were obtained from a Shimadzu LCMS-IT-TOF system (Shimadzu, Kyoto, Japan).

2.2. General procedure for the preparation of ethyl 2-[(1-methyl/phenyl-1*H*-tetrazol-5-yl)thio] acetate

A mixture of 5-mercapto-1-methyl/phenyl-1*H*-tetrazole (0.05 mol) and ethyl chloroacetate (0.05 mol) in the presence of potassium carbonate (0.05 mol) in acetone was refluxed for 10 h. Upon completion of the reaction, the solvent was evaporated. The crude product was solved in water and then extracted with diethyl ether. After extraction, the solvent was evaporated [26,27].

2.3. General procedure for the preparation of 2-[(1-methyl/phenyl-1*H*-tetrazol-5-yl)thio)] acetohydrazide

A mixture of the appropriate ester (0.05 mol) and hydrazine hydrate (0.1 mol) in ethanol was stirred at room temperature for 3 h [26,27]. Upon completion of the reaction, the precipitate was collected by filtration and dried.

2.4. General procedure for the preparation of 2-[(1-methyl/phenyl-1*H*-tetrazol-5-yl)thio]-*N*'-(4-substituted benzylidene) acetohydrazides (1-12)

A mixture of the appropriate hydrazide (0.01 mol) and aromatic aldehydes (0.01 mol) was refluxed in ethanol for 7 h. Upon completion of the reaction, the precipitate was collected by filtration and dried. The product was crystallized from ethanol.

2.4.1. 2-[(1-Methyl-1H-tetrazol-5-yl)thio]-N'-(4-(piperidin-1-yl)benzylidene)acetohydrazide (1)

M.p.: 138.4 °C. Yield: 84%.

^{1}H NMR (300 MHz, DMSO-d_6): 1.57 (brs, 6H), 3.25 (brs, 4H), 3.98 (s, 3H), 4.14 and 4.57 (2s, 2H), 6.95 (d, *J*= 8.91 Hz, 2H), 7.49 (dd, *J*= 2.37 Hz, 2.49 Hz, 8.94 Hz, 2H), 7.89 and 8.03 (2s, 1H), 11.51 (s, 1H).

^{13}C NMR (75 MHz, DMSO-d_6): 24.39 (CH_2), 25.42 ($2CH_2$), 34.13 (CH_3), 36.37 (CH_2), 48.81 (CH_2),

48.87 (CH_2), 114.97 (CH), 115.09 (CH), 123.40 (C), 128.64 (CH), 128.93 (CH), 145.05 (CH), 148.20 (C), 152.84 (C), 167.96 (C).

HRMS (ESI) (*m/z*): $[M+H]^+$ calcd. for $C_{16}H_{21}N_7OS$: 360.1601, found: 360.1596.

2.4.2. 2-[(1-Methyl-1H-tetrazol-5-yl)thio]-N'-(4-(morpholin-4-yl)benzylidene)acetohydrazide (2)

M.p.: 199.2 °C. Yield: 90%.

^{1}H NMR (300 MHz, DMSO-d_6): 3.19-3.21 (m, 4H), 3.72-3.75 (m, 4H), 3.98 (s, 3H), 4.15 and 4.58 (2s, 2H), 6.98 (d, *J*= 8.79 Hz, 2H), 7.54 (dd, *J*= 2.43 Hz, 2.58 Hz, 8.90 Hz, 2H), 7.92 and 8.06 (2s, 1H), 11.54 (s, 1H).

^{13}C NMR (75 MHz, DMSO-d_6): 34.11 (CH_3), 36.34 (CH_2), 47.86 (CH_2), 47.92 (CH_2), 66.40 ($2CH_2$), 114.74 (CH), 114.83 (CH), 124.57 (C), 128.56 (CH), 128.84 (CH), 144.88 (CH), 148.04 (C), 152.64 (C), 168.05 (C).

HRMS (ESI) (*m/z*): $[M+H]^+$ calcd. for $C_{15}H_{19}N_7O_2S$: 362.1394, found: 362.1387.

2.4.3. 2-[(1-Methyl-1H-tetrazol-5-yl)thio]-N'-(4-(4-methylpiperazin-1-yl)benzylidene)acetohydrazide (3)

M.p.: 139.2 °C. Yield: 88%.

^{1}H NMR (300 MHz, DMSO-d_6): 2.21 (s, 3H), 2.41-2.43 (m, 4H), 3.21-3.24 (m, 4H), 3.98 (s, 3H), 4.15 and 4.57 (2s, 2H), 6.97 (d, *J*= 8.76 Hz, 2H), 7.52 (dd, *J*= 3.12 Hz, 3.15 Hz, 8.84 Hz, 2H), 7.90 and 8.04 (2s, 1H), 11.52 (s, 1H).

^{13}C NMR (75 MHz, DMSO-d_6): 34.13 (CH_3), 36.35 (CH_2), 46.21 (CH_3), 47.51 (CH_2), 47.57 (CH_2), 54.87 ($2CH_2$), 114.89 (CH), 114.98 (CH), 124.08 (C), 128.57 (CH), 128.85 (CH), 144.96 (CH), 148.10 (C), 152.53 (C), 168.01 (C).

HRMS (ESI) (*m/z*): $[M+H]^+$ calcd. for $C_{16}H_{22}N_8OS$: 375.1710, found: 375.1712.

2.4.4. 2-[(1-Methyl-1H-tetrazol-5-yl)thio]-N'-(4-(pyrrolidin-1-yl)benzylidene)acetohydrazide (4)

M.p.: 203.4 °C. Yield: 82%.

^{1}H NMR (300 MHz, DMSO-d_6): 1.93-1.97 (m, 4H), 3.25-3.29 (m, 4H), 3.98 (s, 3H), 4.13 and 4.56 (2s, 2H), 6.56 (d, *J*= 8.76 Hz, 2H), 7.48 (dd, *J*= 3.09 Hz, 3.12 Hz, 8.75 Hz, 2H), 7.87 and 8.01 (2s, 1H), 11.42 (s, 1H).

^{13}C NMR (75 MHz, DMSO-d_6): 25.41 ($2CH_2$), 34.10 (CH_3), 36.40 (CH_2), 47.69 ($2CH_2$), 112.00 (2CH), 120.94 (C), 128.84 (CH), 129.13 (CH), 145.63 (CH), 148.81 (C), 149.32 (C), 167.77 (C).

HRMS (ESI) (*m/z*): $[M+H]^+$ calcd. for $C_{15}H_{19}N_7OS$: 346.1445, found: 346.1428.

2.4.5. 2-[(1-Methyl-1H-tetrazol-5-yl)thio]-N'-(4-(1H-imidazol-1-yl)benzylidene)acetohydrazide (5)

M.p.: 191.1 °C. Yield: 88%.

^{1}H NMR (300 MHz, DMSO-d_6): 3.99 (s, 3H), 4.20 and 4.63 (2s, 2H), 7.14 (brs, 1H), 7.76 (d, *J*= 8.76 Hz, 2H), 7.82-7.85 (m, 3H), 8.06 and 8.23 (2s, 1H), 8.35 (brs, 1H), 11.81 and 11.85 (2s, 1H).

^{13}C NMR (75 MHz, DMSO-d_6): 34.13 (CH_3), 36.19 (CH_2), 118.26 (CH), 120.79 (2CH), 128.86 (CH), 129.08 (CH), 130.63 (CH), 132.76 (C), 136.02 (CH), 138.29 (C), 143.45 (CH), 146.72 (C), 168.60 (C).

HRMS (ESI) (*m/z*): $[M+H]^+$ calcd. for $C_{14}H_{14}N_8OS$: 343.1084, found: 343.1074.

2.4.6. 2-[(1-Methyl-1H-tetrazol-5-yl)thio]-N'-(4-(1H-1,2,4-triazol-1-yl)benzylidene)acetohydrazide (6)

M.p.: 257.9 °C. Yield: 86%.

^{1}H NMR (300 MHz, DMSO-d_6): 3.99 (s, 3H), 4.20 and 4.64 (2s, 2H), 7.88 (d, *J*= 8.64 Hz, 2H), 7.96 (d, *J*= 8.73 Hz, 2H), 8.07 and 8.24 (2s, 1H), 8.27 (s, 1H), 9.37 (s, 1H), 11.84 (s, 1H).

^{13}C NMR (75 MHz, DMSO-d_6): 34.14 (CH_3), 36.17 (CH_2), 120.00 (2CH), 128.78 (CH), 129.00 (CH), 133.67 (C), 137.99 (C), 142.96 (CH), 143.36 (CH), 146.54 (CH), 153.07 (C), 168.62 (C).

HRMS (ESI) (*m/z*): $[M+H]^+$ calcd. for $C_{13}H_{13}N_9OS$: 344.1037, found: 344.1028.

2.4.7. 2-[(1-Phenyl-1H-tetrazol-5-yl)thio]-N'-(4-(piperidin-1-yl)benzylidene)acetohydrazide (7)

M.p.: 189.4 °C. Yield: 83%.

^{1}H NMR (300 MHz, DMSO-d_6): 1.56 (brs, 6H), 3.24 (brs, 4H), 4.28 and 4.69 (2s, 2H), 6.94 (dd, *J*= 2.37 Hz, 2.64 Hz, 8.99 Hz, 2H), 7.50 (dd, *J*= 3.63 Hz, 3.66 Hz, 8.75 Hz, 2H), 7.65-7.68 (m, 5H), 7.91 and 8.06 (2s, 1H), 11.55 and 11.59 (2s, 1H).

^{13}C NMR (75 MHz, DMSO-d_6): 24.38 (CH_2), 25.42 ($2CH_2$), 36.72 (CH_2), 48.87 ($2CH_2$), 114.96 (CH), 115.08 (CH), 123.39 (C), 124.91 (2CH), 128.63 (CH), 128.94 (CH), 130.53 (2CH), 131.09 (CH), 133.57 (C), 145.16 (CH), 148.24 (C), 152.84 (C), 167.71 (C).

HRMS (ESI) (*m/z*): $[M+H]^+$ calcd. for $C_{21}H_{23}N_7OS$: 422.1758, found: 422.1756.

2.4.8. 2-[(1-Phenyl-1H-tetrazol-5-yl)thio]-N'-(4-(morpholin-4-yl)benzylidene)acetohydrazide (8)

M.p.: 251.6 °C. Yield: 89%.

^{1}H NMR (300 MHz, DMSO-d_6): 3.20 (brs, 4H), 3.74 (brs, 4H), 4.27 and 4.69 (2s, 2H), 6.99 (d, *J*= 8.25 Hz, 2H), 7.54 (d, *J*= 6.90 Hz, 2H), 7.69 (brs, 5H), 7.92 and 8.07 (2s, 1H), 11.58 and 11.62 (2s, 1H).

^{13}C NMR (75 MHz, DMSO-d_6): 36.68 (CH_2), 47.91 ($2CH_2$), 66.40 ($2CH_2$), 114.75 (CH), 114.84 (CH), 124.55 (C), 124.95 (2CH), 128.56 (CH), 128.84 (CH), 130.54 (2CH), 131.12 (CH), 133.57 (C), 144.99 (CH), 148.24 (C), 152.84 (C), 167.71 (C).

HRMS (ESI) (*m/z*): $[M+H]^+$ calcd. for $C_{20}H_{21}N_7O_2S$: 424.1550, found: 424.1551.

2.4.9. 2-[(1-Phenyl-1H-tetrazol-5-yl)thio]-N'-(4-(4-methylpiperazin-1-yl)benzylidene)acetohydrazide (9)

M.p.: 209.2 °C. Yield: 87%.

^{1}H NMR (300 MHz, DMSO-d_6): 2.21 (s, 3H), 2.43 (brs, 4H), 3.21-3.23 (m, 4H), 4.27 and 4.69 (2s, 2H), 6.97 (dd, *J*= 2.34 Hz, 2.43 Hz, 8.87 Hz, 2H), 7.52 (dd, *J*= 2.97 Hz, 8.76 Hz, 2H), 7.69-7.71 (m, 5H), 7.91 and 8.06 (2s, 1H), 11.56 and 11.61 (2s, 1H).

^{13}C NMR (75 MHz, DMSO-d_6): 36.67 (CH_2), 46.20 (CH_3), 47.55 ($2CH_2$), 54.85 ($2CH_2$), 114.89 (CH), 114.99 (CH), 124.07 (C), 124.94 (2CH), 128.57 (CH), 128.86 (CH), 130.54 (2CH), 131.12 (CH), 133.56 (C), 145.06 (CH), 148.12 (C), 152.54 (C), 167.76 (C).

HRMS (ESI) (*m/z*): $[M+H]^+$ calcd. for $C_{21}H_{24}N_8OS$: 437.1867, found: 437.1884.

2.4.10. 2-[(1-Phenyl-1H-tetrazol-5-yl)thio]-N'-(4-(pyrrolidin-1-yl)benzylidene)acetohydrazide (10)

M.p.: 215.1 °C. Yield: 81%.

^{1}H NMR (300 MHz, DMSO-d_6): 1.95 (brs, 4H), 3.27 (brs, 4H), 4.26 and 4.68 (2s, 2H), 6.57 (d, *J*= 8.67 Hz, 2H), 7.48 (d, *J*= 8.67 Hz, 2H), 7.69 (brs, 5H), 7.88 and 8.03 (2s, 1H), 11.47 and 11.50 (2s, 1H).

^{13}C NMR (75 MHz, DMSO-d_6): 25.41 ($2CH_2$), 36.73 (CH_2), 47.68 ($2CH_2$), 112.01 (2CH), 120.92 (C), 124.94 (2CH), 128.83 (CH), 129.14 (CH), 130.53 (2CH), 131.10 (CH), 133.57 (C), 145.72 (CH), 148.83 (C), 149.33 (C), 167.53 (C).

HRMS (ESI) (*m/z*): $[M+H]^+$ calcd. for $C_{20}H_{21}N_7OS$: 408.1601, found: 408.1604.

2.4.11. 2-[(1-Phenyl-1H-tetrazol-5-yl)thio]-N'-(4-(1H-imidazol-1-yl)benzylidene)acetohydrazide (11)

M.P.: 236.4 °C. Yield: 86%.

^{1}H NMR (300 MHz, DMSO-d_6): 4.32 and 4.75 (2s, 2H), 7.14 (brs, 1H), 7.65-7.71 (m, 5H), 7.76 (d, *J*= 8.70 Hz, 2H), 7.84 (d, *J*= 8.70 Hz, 3H), 8.07 and 8.25 (2s, 1H), 8.36 (brs, 1H), 11.86 and 11.92 (2s, 1H).

^{13}C NMR (75 MHz, DMSO-d_6): 36.54 (CH_2), 118.29 (CH), 120.80 (2CH), 124.92 (2CH), 128.84 (CH), 129.08 (CH), 130.55 (2CH), 131.13 (CH), 132.75 (CH), 132.83 (C), 133.55 (C), 136.02 (CH), 138.30 (C), 143.56 (CH), 146.75 (C), 168.35 (C).

HRMS (ESI) (*m/z*): $[M+H]^+$ calcd. for $C_{19}H_{16}N_8OS$: 405.1241, found: 405.1250.

2.4.12. 2-[(1-Phenyl-1H-tetrazol-5-yl)thio]-N'-(4-(1H-1,2,4-triazol-1-yl)benzylidene)acetohydrazide (12)

M.p.: 240.6 °C. Yield: 84%.

^{1}H NMR (300 MHz, DMSO-d_6): 4.32 and 4.75 (2s, 2H), 7.67-7.70 (m, 5H), 7.89 (d, *J*= 8.73 Hz, 2H), 7.96 (d, *J*= 8.49 Hz, 2H), 8.09 and 8.26 (2s, 1H), 8.28 (s, 1H), 9.38 (s, 1H), 11.88 (s, 1H).

^{13}C NMR (75 MHz, DMSO-d_6): 36.48 (CH_2), 120.02 (2CH), 124.94 (2CH), 128.77 (CH), 129.01 (CH), 130.56 (2CH), 131.14 (CH), 133.55 (C), 133.66 (C), 138.01 (C), 142.96 (CH), 143.46 (CH), 146.58 (CH), 153.07 (C), 168.36 (C).

HRMS (ESI) (*m/z*): $[M+H]^+$ calcd. for $C_{18}H_{15}N_9OS$: 406.1193, found: 406.1195.7

2.5. Biochemistry

2.5.1. Determination of COX inhibitory potency

COX colorimetric inhibitor screening assay kit (item no: 701050), which includes both ovine COX-1 and human recombinant COX-2, is used to measure the peroxidase component of COXs. In this method, the peroxidase activity is detected colorimetrically *via* monitoring the appearance of oxidized *N,N,N',N'*-tetramethyl-*p*-phenylenediamine (TMPD) at 590 nm.

In the current work, this kit was applied to determine the inhibitory activities of compounds **1-12** (at 100 μM) towards both COXs according to the manufacturer's instructions (Cayman, Ann Arbor, MI, USA). All measurements were performed in triplicate and the data were expressed as mean ± SD. SC-560 (at 1 μM) was used as a selective COX-1 inhibitor, whilst rofecoxib (at 10 μM) was used as a selective COX-2 inhibitor.

3. RESULTS AND DISCUSSION

3.1. Chemistry

The synthesis of the hitherto unreported compounds (**1-12**) was performed as depicted in Figure 1. Ethyl 2-[(1-methyl/phenyl-1*H*-tetrazol-5-yl)thio]acetate was prepared *via* the treatment of 5-mercapto-1-methyl/phenyl-1*H*-tetrazole with ethyl chloroacetate in the presence of potassium carbonate. The reaction of this ester with hydrazine hydrate yielded 2-[(1-methyl/phenyl-1*H*-tetrazol-5-yl)thio)] acetohydrazide, which underwent a subsequent nucleophilic addition-elimination reaction with aromatic aldehydes affording compounds **1-12**. Their structures were confirmed by ^{1}H and ^{13}C NMR, HRMS data. In the ^{1}H NMR spectra of compounds **1-12**, the signal due to CH=N proton was detected in the region 7.87-8.26 ppm as two singlets. The signal due to N-H proton appeared in the region 11.42-11.92 ppm as a singlet or two singlets. The

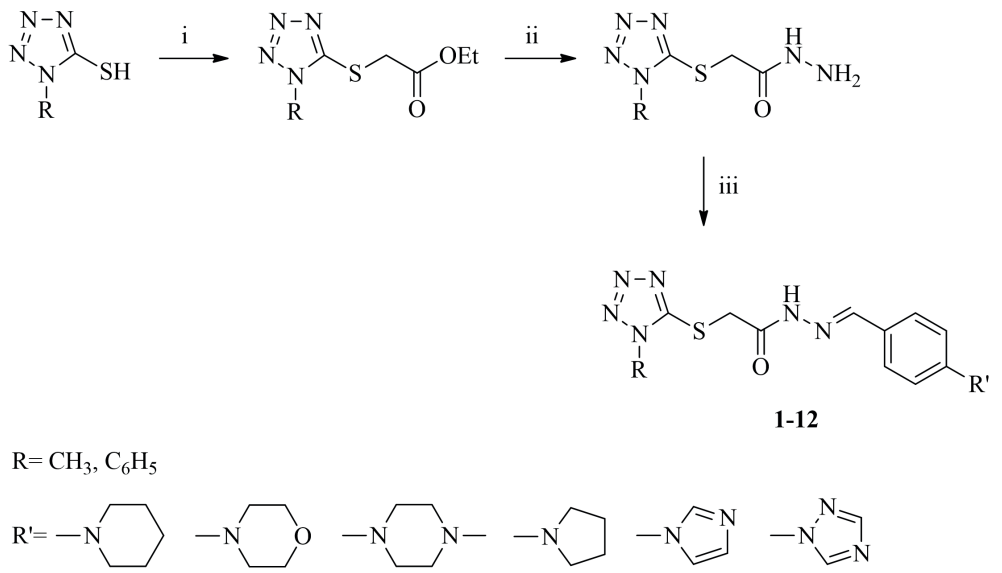

Figure 1. The synthetic route for the preparation of compounds **1-12**. Reagents and conditions: (i) $ClCH_2COOEt$, K_2CO_3, acetone, reflux, 10h; (ii) $NH_2NH_2.H_2O$, ethanol, rt, 3h; (iii) ArCHO, ethanol, reflux, 7h.

signal due to the S-CH_2 protons was observed as two singlets in the region 4.13-4.75 ppm. In the ^{1}H NMR spectra of compounds **1-6**, the protons of the methyl group attached to the *N*1 atom of the tetrazole ring gave rise to a singlet peak at 3.98-3.99 ppm. In the ^{13}C NMR spectra of compounds **1-12**, the signal due to the CH=N carbon was observed at 143.45-146.58 ppm, whereas the signal due to the C=O carbon was detected in the region 167.53-168.62 ppm. The S-CH_2 carbon gave rise to a singlet peak at 36.17-36.73 ppm. In the ^{13}C NMR spectra of compounds **1-6**, the methyl carbon attached to the *N*1 atom of the tetrazole ring gave rise to a singlet peak at 34.10-34.14 ppm. The HRMS data were also in agreement with the proposed structures of compounds **1-12**.

3.2. *In vitro* COX inhibition

A colorimetric assay was employed to assess the COX inhibitory profiles of compounds **1-12** (Table 1). Compounds **7** and **11** did not show any inhibitory activity towards COXs. Compounds **3**, **8**, **9** and **12** showed inhibitory activity towards both COXs. Among them, compound **3** preferentially inhibited COX-1, whilst compounds **8** and **9** preferentially inhibited COX-2. Compound **12** showed nonselective COX inhibitory activity and its inhibitory effects on COX-1 and COX-2 were found to be insignificant. The 1,2,4-triazole ring at the 4th position of the benzylidene motif caused a diminution in COX inhibitory potency.

The most potent and selective COX-1 inhibitors were found as compounds **1** (40.88±2.79%) and **2** (39.80±2.78%) carrying 1-methyl-1*H*-tetrazole moiety as compared to SC-560 (97.36±2.62%). These compounds did not show any inhibitory activity towards COX-2. The replacement of the methyl group of compound **1** with the phenyl moiety of compound **7** resulted in the loss of COX-1 inhibitory activity as well as COX-2 inhibitory potency. The replacement of the methyl group of compound **2** with the phenyl moiety of compound **8** led to a decrease in COX-1 inhibitory potency

Table 1. COX inhibition (%) caused by compounds **1-12** and reference agents

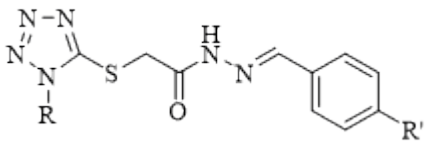

Compound (100 µM)	R	R'	Inhibition%	
			COX-1	COX-2
1	CH_3	Piperidin-1-yl	40.88±2.79	----
2	CH_3	Morpholin-4-yl	39.80±2.78	----
3	CH_3	4-Methylpiperazin-1-yl	27.97±2.69	12.45±1.22
4	CH_3	Pyrrolidin-1-yl	35.36±3.93	----
5	CH_3	1*H*-Imidazol-1-yl	33.41±3.09	----
6	CH_3	1*H*-1,2,4-Triazol-1-yl	19.55±1.96	----
7	C_6H_5	Piperidin-1-yl	----	----
8	C_6H_5	Morpholin-4-yl	14.37±2.31	30.26±0.76
9	C_6H_5	4-Methylpiperazin-1-yl	21.77±1.58	38.82±0.24
10	C_6H_5	Pyrrolidin-1-yl	----	42.38±1.16
11	C_6H_5	1*H*-Imidazol-1-yl	----	----
12	C_6H_5	1*H*-1,2,4-Triazol-1-yl	9.86±3.06	12.46±1.46
SC-560 (1 µM)	-	-	97.36±2.62	ND
Rofecoxib (10 µM)	-	-	ND	98.36±1.86

ND: Not determined.

(14.37±2.31%) and a substantial increase in COX-2 inhibitory activity (30.26±0.76%).

The most potent COX-2 inhibitors were found as compounds **10** (42.38±1.16%) and **9** (38.82±0.24%) carrying 1-phenyl-1*H*-tetrazole moiety as compared to rofecoxib (98.36±1.86%). Compound **9** also inhibited COX-1 (21.77±1.58%), whilst compound **10** did not show any inhibitory potency on COX-1.

In general, 1-methyl-1*H*-tetrazole moiety gave rise to selective COX-1 inhibition, whereas 1-phenyl-1*H*-tetrazole moiety led to preferential COX-2 inhibition. It can be concluded that the substituent at the 1st position of the tetrazole ring is of great importance for selectivity. The replacement of the alkyl (methyl) group with the bulky aryl moiety shifted the selective inhibition from COX-1 to COX-2.

4. CONCLUSION

In this paper, we conducted a simple and efficient protocol for the preparation of a series of tetrazole-based hydrazones (**1-12**), which were investigated for their inhibitory effects on COXs at 100 μM using an *in vitro* colorimetric assay. Based on *in vitro* experimental data, compounds **1** (40.88±2.79%) and **2** (39.80±2.78%) carrying 1-methyl-1*H*-tetrazole moiety were found as the most potent and selective COX-1 inhibitors. On the other hand, compound **10** (42.38±1.16%) carrying 1-phenyl-1*H*-tetrazole moiety was determined as the most potent and selective COX-2 inhibitor in this series. This work could represent a rational guideline for further structural modifications to generate a new class of tetrazole-based hydrazones endowed with selective COX-1 or COX-2 inhibitory activity.

Ethical approval

Not applicable, because this article does not contain any studies with human or animal subjects.

Author contribution

Concept: MDA, ZAK and AÖ; Design: MDA and ZAK; Materials: MDA, BS, HET, ZAK and AÖ; Data Collection and/or Processing: MDA, BS and HET; Analysis and/or Interpretation: MDA and HET; Literature Search: MDA; Writing: MDA; Critical Reviews: MDA, BS, HET, ZAK and AÖ.

Source of funding

This study was supported by Anadolu University Scientific Research Projects Commission under the grant no: 2005S019.

Conflict of interest

The authors declare that there is no conflict of interest.

REFERENCES

1. Rouzer CA, Marnett LJ. Structural and chemical biology of the interaction of cyclooxygenase with substrates and non-steroidal anti-inflammatory drugs. Chem Rev. 2020;120:7592-7641. https://dx.doi.org/10.1021/acs.chemrev.0c00215
2. Brock TG, McNish RW, Peters-Golden M. Arachidonic acid is preferentially metabolized by cyclooxygenase-2 to prostacyclin and prostaglandin E2. J Biol Chem. 1999;274(17):11660-11666. https://doi.org/10.1074/jbc.274.17.11660
3. Mazaleuskaya LL, Ricciotti E. Druggable prostanoid pathway. Adv Exp Med Biol. 2020;1274:29-54. https://doi.org/10.1007/978-3-030-50621-6_3
4. Pannunzio A, Coluccia M. Cyclooxygenase-1 (COX-1) and COX-1 inhibitors in cancer: A review of oncology and medicinal chemistry literature. Pharmaceuticals (Basel). 2018;11(4):101. https://doi.org/10.3390/ph11040101
5. Sharma V, Bhatia P, Alam O, et al. Recent advancement in the discovery and development of COX-2 inhibitors: Insight into biological activities and SAR studies (2008-2019). Bioorg Chem. 2019;89:103007. https://doi.org/10.1016/j.bioorg.2019.103007

6. Zidar N, Odar K, Glavac D, Jerse M, Zupanc T, Stajer D. Cyclooxygenase in normal human tissues – is COX-1 really a constitutive isoform, and COX-2 an inducible isoform? J Cell Mol Med. 2009;13:3753-3763. https://doi.org/10.1111/j.1582-4934.2008.00430.x

7. Yu T, Lao X, Zheng H. Influencing COX-2 activity by COX related pathways in inflammation and cancer. Mini Rev Med Chem. 2016;16:1230-1243. https://doi.org/10.2174/1389557516666160505115743

8. Gandhi J, Khera L, Gaur N, Paul C, Kaul R. Role of modulator of inflammation cyclooxygenase-2 in gammaherpesvirus mediated tumorigenesis. Front Microbiol. 2017;8:538. https://doi.org/10.3389/fmicb.2017.00538

9. Caiazzo E, Ialenti A, Cicala C. The relatively selective cyclooxygenase-2 inhibitor nimesulide: What's going on? Eur J Pharmacol. 2019;848:105-111. https://doi.org/10.1016/j.ejphar.2019.01.044

10. Vitale P, Tacconelli S, Perrone MG, et al. Synthesis, pharmacological characterization, and docking analysis of a novel family of diarylisoxazoles as highly selective cyclooxygenase-1 (COX-1) inhibitors. J Med Chem. 2013;56(11):4277-4299. https://doi.org/10.1021/jm301905a

11. Perrone MG, Scilimati A, Simone L, Vitale P. Selective COX-1 inhibition: A therapeutic target to be reconsidered. Curr Med Chem. 2010;17(32):3769-3805. https://doi.org/10.2174/092986710793205408

12. Carullo G, Galligano F, Aiello F. Structure-activity relationships for the synthesis of selective cyclooxygenase 2 inhibitors: An overview (2009-2016). Medchemcomm. 2016;8(3):492-500. https://doi.org/10.1039/c6md00569a

13. Kumar P, Narasimhan B. Hydrazides/hydrazones as antimicrobial and anticancer agents in the new millennium. Mini-Rev Med Chem. 2013;13:971-987. https://doi.org/10.2174/1389557511313070003

14. Rollas S, Küçükgüzel SG. Biological activities of hydrazone derivatives. Molecules. 2007;12(8):1910-1939. https://doi.org/10.3390/12081910

15. Narang R, Narasimhan B, Sharma S. A review on biological activities and chemical synthesis of hydrazide derivatives. Curr Med Chem. 2012;19(4):569-612. https://10.2174/092986712798918789

16. Mali SN, Thorat BR, Gupta DR, Pandey A. Mini-review of the importance of hydrazides and their derivatives—Synthesis and biological activity. Eng Proc. 2021;11:21. https://doi.org/10.3390/ASEC2021-11157

17. Ju Z, Su M, Hong J, et al. Design of balanced COX inhibitors based on anti-inflammatory and/or COX-2 inhibitory ascidian metabolites. Eur J Med Chem. 2019;180:86-98. https://doi.org/10.1016/j.ejmech.2019.07.016

18. Abdelgawad MA, Labib MB, Abdel-Latif M. Pyrazole-hydrazone derivatives as anti-inflammatory agents: Design, synthesis, biological evaluation, COX-1,2/5-LOX inhibition and docking study. Bioorg Chem. 2017;74:212-220. https://doi.org/10.1016/j.bioorg.2017.08.014

19. Gorantla V, Gundla R, Jadav SS, et al. Molecular hybrid design, synthesis and biological evaluation of *N*-phenyl sulfonamide linked *N*-acyl hydrazone derivatives functioning as COX-2 inhibitors: new anti-inflammatory, anti-oxidant and anti-bacterial agents. New J Chem. 2017;41:13516-13532. https://doi.org/10.1039/c7nj03332j

20. Mohammed KO, Nissan YM. Synthesis, molecular docking, and biological evaluation of some novel hydrazones and pyrazole derivatives as anti-inflammatory agents. Chem Biol Drug Des. 2014;84(4):473-488. https://doi.org/10.1111/cbdd.12336

21. El-Sayed MA, Abdel-Aziz NI, Abdel-Aziz AA, El-Azab AS, Asiri YA, Eltahir KE. Design, synthesis, and biological evaluation of substituted hydrazone and pyrazole derivatives as selective COX-2 inhibitors: Molecular docking study. Bioorg Med Chem. 2011;19(11):3416-3424. https://doi.org/10.1016/j.bmc.2011.04.027

22. Xiong Q, Dong S, Chen Y, Liu X, Feng X. Asymmetric synthesis of tetrazole and dihydroisoquinoline derivatives by isocyanide-based multicomponent reactions. Nat Commun. 2019;10(1):2116. https://doi.org/10.1038/s41467-019-09904-5

23. Lamie PF, Philoppes JN, Azouz AA, Safwat NM. Novel tetrazole and cyanamide derivatives as inhibitors of cyclooxygenase-2 enzyme: design, synthesis, anti-inflammatory evaluation, ulcerogenic liability and docking study. J Enzyme Inhib Med Chem. 2017;32:805-820. https://doi.org/10.1080/14756366.2017.1326110

24. Labib MB, Fayez AM, El-Nahass ES, Awadallah M, Halim PA. Novel tetrazole-based selective COX-2 inhibitors: Design, synthesis, anti-inflammatory activity, evaluation of PGE2, TNF-α, IL-6 and histopathological study. Bioorg Chem. 2020;104:104308. https://doi.org/10.1016/j.bioorg.2020.104308

25. Wei CX, Bian M, Gong GH. Tetrazolium compounds: synthesis and applications in medicine. Molecules. 2015;20(4):5528-5553. https://doi.org/10.3390/molecules20045528

26. Altıntop MD, Kaplancıklı ZA, Akalın Çiftçi G, Demirel R. Synthesis and biological evaluation of thiazoline derivatives as new antimicrobial and anticancer agents. Eur J Med Chem. 2014;74:264-277. https://doi.org/10.1016/j.ejmech.2013.12.060

27. Altıntop MD, Özdemir A, Turan-Zitouni G, et al. Synthesis and biological evaluation of some hydrazone derivatives as new anticandidal and anticancer agents. Eur J Med Chem. 2012;58:299-307. https://doi.org/10.1016/j.ejmech.2012.10.011

ANADOLU UNIVERSITY
INSTITUTE OF HEALTH SCIENCES

European Journal of Life Sciences 2022; 1: 28-34

Research Article

Chaerophyllum libanoticum Boiss. Et Kotschy: The fruit essential oil, composition, skin-whitening and antioxidant activities

Mine Kürkçüoğlu[1]✉, Hale Gamze Ağalar[1], Burak Temiz[1], Ahmet Duran[2], Kemal Hüsnü Can Başer[3]

[1]Department of Pharmacognosy, Faculty of Pharmacy, Anadolu University, 26470, Eskisehir, Turkey.
[2]Emeritus Professor, Department of Biology, Faculty of Science, Selçuk University, 42075, Konya, Turkey.
[3]Department of Pharmacognosy, Faculty of Pharmacy, Near East University, Nicosia, North Cyprus.

✉ Mine Kürkçüoğlu
mkurkucuo@anadolu.edu.tr

https://doi.org/10.55971/EJLS.1095855

Received: 03.30.2022
Accepted: 04.26.2022
Available online: 06.06.2022

ABSTRACT

This study was aimed to evaluate the essential oil composition of *Chaerophyllum libanoticum* fruits and its potential uses in the cosmetic industry. The essential oil was analyzed by Gas Chromatography and Gas Chromatography-Mass Spectrometry (GC-GC/MS) systems, simultaneously. The yield of essential oil was calculated as 0.22 % (*v/w*). Major components of the oil were characterized as limonene (26.7%), *p*-cymene (25.5%), and β-phellandrene (7.0%). In addition, antioxidant and antityrosinase activities of the essential oil were evaluated. The oil exhibited moderate antioxidant activity (TEAC). In the DPPH$^{\bullet}$ assay, the oil was tested at 5 mg/mL concentration, and the inhibition ratio was calculated as 31.3 ± 1.1%. At 1 mg/mL of concentration, TEAC (mmol/L) value was determined as 0.027 ± 0.008. As evidence to its skin whitening properties, the oil inhibited the tyrosinase 17.7 ± 1.6 % at 1 mg/mL..

Keywords: *Chaerophyllum libanoticum*, Apiaceae, Essential oil, Antioxidant, Antityrosinase

1. INTRODUCTION

Apiaceae is considered as one of the most important families due to its economic value in the field of pharmaceutical, cosmetic, flavor, and fragrance industries and is represented by about 3780 species in 434 genera [1,2]. The genus *Chaerophyllum* L. is represented in the Flora of Turkey by 15 species [3], and the members of the genus have a distinctive aromatic character [4]. *Chaerophyllum* Boiss. et Kotschy. is known as "Mentik" in Southern parts of Turkey, and is consumed as food like some other *Chaerophyllum* species [5].

Essential oil components are responsible for the characteristic fragrance of *Chaerophyllum* species, and various studies have been reported on the volatile composition of different parts and origins [6-11]. Previous investigations on biological properties of *Chaerophyllum* species revealed that they possess various biological activities such as antimicrobial [7,10], antioxidant [7,10], anti-inflammatory [7], angiotensin-converting enzyme (ACE) inhibition [12], glutathione-*S*-transferase inhibition [13], cytotoxic properties [14].

Essential oils have been used in cosmetic preparations due to their health benefit effects in skin disorders related to their antioxidant, antimicrobial and anti-inflammatory activities. Recently, tyrosinase, a key enzyme in the production of melanin, has become

one of the most important targets in the cosmetic industry [15]. Overproduction of melanin leads to hyperpigmentation, age spots, melasma, and this process might be related to increased oxidative stress on the skin. Essential oils, their components and essential oil-bearing plants are considered natural cosmetic ingredients. They may also possess antioxidant and antityrosinase properties.

This present study was aimed to characterize volatile constituents of *Chaerophyllum libonoticum* Boiss. Et Kotschy fruit essential oil collected from Osmaniye. The essential oil was analyzed by GC-FID and GC/MS system, simultaneously. Furthermore, antioxidant and antityrosinase activities were determined by *in vitro* methods.

2. MATERIALS AND METHODS

2.1. Plant Material

Chaerophyllum libanoticum was collected from Osmaniye; Zorkun, Mitisin Plateau at an altitude 1340 m in Turkey, on October 14, 2018 (Ahmet Duran, 10733).

2.2. Chemicals and Reagents

All chemicals and solvents were of high purity and at least of analytical grade. 1,1- diphenyl-2-picrylhydrazyl (DPPH$^{\bullet}$) (Aldrich), 2,2'-azinobis-(3-ethylbenzothiazoline)-6-sulfonic acid (Sigma-Aldrich), Trolox ((*S*)-6-hydroxy-2,5,7,8-tetramethylchromane-2-carboxylic acid, Sigma-Aldrich), gallic acid (Sigma), ascorbic acid (Sigma-Aldrich), L-DOPA (Sigma), kojic acid (Sigma-Aldrich), tyrosinase from mushroom (Sigma-Aldrich), dipotassium hydrogen phosphate (Merck), sodium dihydrogen phosphate dihydrate (Merck), sodium sulfate anhydrous (Sigma-Aldrich), potassium persulfate (Sigma-Aldrich), methanol (Merck), ethanol (Sigma-Aldrich), and *n*-hexane (Sigma-Aldrich) were purchased.

2.3. Isolation of Essential Oil

The air-dried fruits of *Chaerophyllum libanoticum* were subjected to hydrodistillation, using a Clevenger-type apparatus for 3h. The obtained oils were kept at +4°C in the dark until the experiments.

2.4. GC-FID Analysis

GC analyses were performed using an Agilent 6890N GC system. FID temperature was set to 300°C and the same operational conditions were applied to a triplicate of the same column used in GC/MS analyses. Simultaneous auto injection was employed to obtain equivalent retention times. Relative percentages of the separated compounds were calculated from integration of the peak areas in the GC-FID chromatograms.

2.5. GC/MS Analysis

The GC/MS analysis was carried out with an Agilent 5975 GC-MSD system (Agilent, USA; SEM Ltd., Istanbul, Turkey). Innowax FSC column (60m x 0.25mm, 0.25µm film thickness) was used with helium as carrier gas (0.8 mL/min.). GC oven temperature was kept at 60°C for 10 min and programmed to 220°C at a rate of 4°C/min, and kept constant at 220°C for 10 min and then programmed to 240°C at a rate of 1°C/min. Split ratio was adjusted 40:1. The injector temperature was at 250°C. The interphase temperature was at 280°C. MS were taken at 70 eV. Mass range was from m/z 35 to 450.

2.6. Identification of Compounds

The components of essential oils were identified by comparison of their mass spectra with those in the in-house Baser Library of Essential Oil Constituents, Adams Library [16], MassFinder Library [17], Wiley GC/MS Library [18], and confirmed by comparison of their retention indices. These identifications were accomplished by comparison of retention times with authentic samples or by comparison of their relative retention index (RRI) to a series of n-alkanes. Alkanes were used as reference points in the calculation of relative retention indices (RRI) [19]. Relative percentage amounts of the separated compounds were calculated from FID chromatograms.

2.7. DPPH Radical Scavenging Activity

DPPH$^{\bullet}$ scavenging activity was determined by the method of Ağalar and Temiz, 2021 [20]. 0.2 mM DPPH solution was prepared in a dark environment with methanol. The experiment was carried out in 96-well microplates. Incubation was carried out for

30 minutes at room temperature and in the dark (A). For the sample control, 100 µL of methanol was added instead of DPPH (B). 0.1 mM DPPH as a blank control (C), methanol (D) as solvent control, and Vitamin C and gallic acid as a positive control were used. Absorbances were measured at 517 nm, and inhibition percentages were calculated according to the formula below (Eq.1).

% inhibition: [(C-D) -(A-B) /(C-D)] x 100 (Eq.1)

2.8. Trolox Equivalent Antioxidant Capacity (TEAC)

The trolox equivalent antioxidant capacity of the essential oils was performed *via* the method described by Re et al. (1999) using $ABTS^{+\bullet}$ radical [21]. 7 mM $ABTS^{+\bullet}$ radical and 2.5 mM potassium persulfate were dissolved in water and kept in the dark for 16h at room temperature. Essential oils were dissolved in ethanol at 1 mg/mL concentration. Trolox were prepared in absolute ethanol with 2.5, 2, 1.5, 1, 0.5, 0.25, 0.125 and 0.0625 mM concentrations. 990 µL $ABTS^{+\bullet}$ solution and 10 µL samples were mixed. Absorbances were measured at 734 nm for 30 min, and the results were expressed as Trolox equivalent antioxidant capacity (mmol/L Trolox).

2.9. Tyrosinase Inhibition

The tyrosinase inhibitory activity of the oil was evaluated by using L-DOPA [20]. Tyrosinase and L-DOPA were prepared in the phosphate buffer (100 mM, pH 6.8). Essential oils were dissolved in buffer containing 5% DMSO. For each sample solution, four wells designated as A, B, C and D each contained a reaction mixture (40 µL) as follows: A, 20 µL buffer (pH 6.8) and 20 µL tyrosinase (200 U/mL); B, 40 µL buffer; C, 20 µL tyrosinase (200 U/mL) and 20 µL sample; D, 20 µL sample and 20 µL buffer. The contents of each well were mixed and incubated at 37 ˚C for 10 min. Then, 5 mM of L-DOPA (160 µL) was added. After second incubation at 37 ˚C for 10 min, the absorbance at 475 nm of each well was measured. The percentage inhibition of the tyrosinase activity was calculated by the following equation 2.

% inhibition: [(A-B)-(C-D)/(A-B)] x 100 (Eq. 2)

2.10. Statistical Analysis

All the experiments were carried out in triplicate, and data were expressed as means ± standard deviation (SD). Statistical analysis were performed using Sigmaplot 14.0 software (Systat Software, Inc., San Jose, CA, USA). IC_{50} values were calculated by regression analysis.

3. RESULTS AND DISCUSSION

3.1. Chemical Composition of *C. libanoticum* Oil

The essential oil obtained from the fruits of *C. libanoticum* was analyzed by GC-GC/MS systems, simultaneously. The essential oil yield was calculated as 0.22% (*v/w*).

Sixty-four constituents were characterized as representing 95.9% of the essential oil. Limonene (26.7%), *p*-cymene (25.5%), and β-phellandrene (7.0%) were found to be the most abundant compounds.

β-Pinene (5.1%), cryptone (4.1%), hexadecanoic acid (3.4%), α-pinene (2.7%), octanal (2.0%), γ-terpinene (1.4%), *trans*-pinocarveol (1.3%), and myrtenol (1.0%) were present in relatively high amounts (Table 1).

In the essential oil, monoterpene hydrocarbons (69.9%) were the most abundant group. Also, the percentage of oxygenated monoterpenes (12.7%) and other compound groups (11.5%) were considerable. In addition, sesquiterpene hydrocarbons (0.7%) and oxygenated sesquiterpenes (1.0%) were present in relatively low amounts. (Figure 1).

Several studies identified essential oil compositions of *Chaerophyllum* species. Previous reports on volatile constituents of *Chaerophyllum* species growing wild in Turkey are given in Table 2. Studies were mainly focused on the aerial parts and fruits of these species. Essential oils obtained from different species were characterized with various major components. Demirci et al. (2007) detected that the fruit essential oil was rich in limonene (15.9 %) and β-phellandrene (17.6 %) [10]. Our results revealed

Table 1. Chemical composition of the fruit essential oil of *C. libanoticum*

RRI	Compounds	%	IM
1032	α-Pinene	2.7	t_R, MS
1118	β-Pinene	5.1	t_R, MS
1132	Sabinene	0.3	t_R, MS
1174	Myrcene	0.1	t_R, MS
1183	Pseudolimonene	0.3	MS
1194	Heptanal	0.2	MS
1203	**Limonene**	**26.7**	t_R, MS
1218	**β-Phellandrene**	**7.0**	t_R, MS
1246	(Z)-β-Ocimene	0.2	t_R, MS
1255	γ-Terpinene	1.4	t_R, MS
1280	***p*-Cymene**	**25.5**	t_R, MS
1290	Terpinolene	0.4	t_R, MS
1296	Octanal	2.0	t_R, MS
1400	Nonanal	0.1	MS
1435	γ -Campholene aldehyde	0.1	MS
1452	*p*-Cymenene	0.2	MS
1458	*cis*-1,2-Limonene epoxide	0.1	MS
1463	Heptanol	0.1	t_R, MS
1468	*trans*-1,2-Limonene epoxide	0.4	MS
1474	*trans*-Sabinene hydrate	0.1	t_R, MS
1476	4,8-Epoxyterpinolene	0.7	MS
1499	α-Campholene aldehyde	0.5	MS
1535	β-Bourbonene	0.2	tR, MS
1548	(*E*)-2-Nonenal	0.8	MS
1553	Linalool	0.5	t_R, MS
1565	8,9-Limonene epoxide-I	0.3	MS
1570	8,9-Limonene epoxide-II	0.1	MS
1571	trans-p-Menth-2-en-1-ol	0.7	MS
1586	Pinocarvone	0.2	MS
1607	Thymol methyl ether	0.1	t_R, MS
1611	Terpinen-4-ol	0.3	t_R, MS
1617	*trans*-Dihydrocarvone	tr	t_R, MS
1638	*trans-p*-Menth-2,8-dien-1-ol / *cis-p*-Menth-2-en-1-ol	0.7	MS
1648	Myrtenal	0.4	MS
1655	(*E*)-2-Decenal	0.3	MS
1670	*trans*-Pinocarveol	1.3	t_R, MS
1678	*cis-p*-Menth-2,8-dien-1-ol	0.5	MS
1690	Cryptone	4.1	MS
1706	α-Terpineol	0.4	t_R, MS
1744	Phellandral	0.7	MS
1751	Carvone	0.8	t_R, MS
1783	β-Sesquiphellandrene	0.2	MS
1786	*ar*-Curcumene	0.3	MS
1804-	Myrtenol	1.0	MS
1811	*trans-p*-Mentha-1(7),8-dien-2-ol	0.3	MS
1815	*p*-Mentha-1,3-dien-7-al	0.1	MS
1845	*trans*-Carveol	0.6	t_R, MS
1864	*p*-Cymen-8-ol	0.9	t_R, MS
1867	*cis*-Carveol	0.3	t_R, MS
1896	*cis-p*-Mentha-1(7),8-dien-2-ol	0.1	MS
2029	Perilla alcohol	0.2	MS
2113	Cumin alcohol	0.3	t_R, MS
2131	Hexahydrofarnesyl acetone	0.2	t_R, MS
2144	Spathulenol	0.2	t_R, MS
2198	Thymol	0.1	t_R, MS
2239	Carvacrol	0.2	t_R, MS
2241	ar-Turmerol	0.2	MS
2278	Torilenol	0.1	MS
2296	Myristicine	0.1	MS
2369	Eudesma-4(15), 7-dien-1β-ol	0.3	MS
2392	Caryophyllenol II	0.2	MS
2931	Hexadecanoic acid	3.4	MS
	Grouped compounds (%)		
	Monoterpene hydrocarbons		69.9
	Oxygenated monoterpenes		12.8
	Sesquiterpene hydrocarbons		0.7
	Oxygenated sesquiterpenes		1.0
	Others		11.5
	TOTAL %		**95.9**

RRI: Relative retention indices calculated against n-alkanes; %: calculated from the FID chromatograms; tr: Trace (<0.1 %). Identification method (IM): t_R, identification based on the retention times (t_R) of genuine compounds on the HP Innowax column; MS, identified on the basis of computer matching of the mass spectra with those of the in-house Baser Library of Essential Oil Constituents, Adams, MassFinder and Wiley libraries and comparison with literature data.

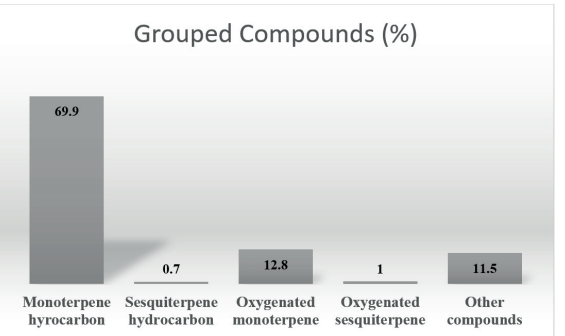

Figure 1. Compound group distribution of the essential oil

Table 2. Main constituents of the essential oils of *Chaerophyllum* species growing wild in Turkey

Plant	Collection place	Parts	Main constituents	Reference
C. aksekiense	Antalya	Fruits	Heptacosane (10.1%), humulene epoxide II (7.8%), (*E*)-β-farnesene (6.2%), caryophyllene oxide (6.0%),	[6]
C. aromaticum	İstanbul	Aerial parts	Sabinene (28.1%), terpinolene (16.7%), γ-terpinene (16.1%)	[7]
C.byzantinum	Bursa	Aerial parts	Sabinene (30.0%), *p*-cymen-8-ol (16.0%), terpinolene (11.5%)	[8]
C. crinitum	Bitlis	Aerial parts	(*E*)-β-Ocimene (38.1%), terpinolene (12.7%)	[9]
C. libanoticum	Osmaniye	Fruits	Limonene (15.9 %), β-phellandrene (17.6 %)	[10]
C. macrospermum	Hakkari	Aerial parts	Terpinolene (21.4%), myristicin (18.9%), *p*-cymen-8-ol (11.9%)	[9]

that the *p*-cymene ratio was higher than that of β-phellandrene. Moreover, Gnannadi et al. (2011) reported that the main constituents of the essential oil obtained from flowering aerial parts of *C. macropodum* were *trans*-β-ocimene (34.5%), *trans*-β-farnesene (11.8%), *cis*-β-ocimene (10.4%), and p-cymene [11]. A study on *C. aromaticum* showed that γ-terpinene (21.0-33.8%), β-phellandrene (14.3-30.0%) and β-pinene (14.3-17.8%) were the main compounds in the fruit essential oil [22].

3.2. Antioxidant Properties of *C. libanoticum* Oil

The antioxidant activity of the essential oil was investigated by two assays, namely DPPH radical scavenging activity and Trolox equivalent antioxidant capacity (TEAC), and the results are given in Table 3. The essential oil of *C. libanoticum* at a 5 mg/mL concentration inhibited DPPH radical by 31.3 ± 1.1 %. The effects were relatively weak when compared with positive controls (vitamin C, IC_{50} value of 9.3 ± 0.01 µg/mL, gallic acid, IC_{50} value of 1.93 ± 0.02 µg/mL). Furthermore, the essential oil presented 0.027 ± 0.008 Trolox equivalent antioxidant capacity at 1 mg/mL concentration.

Demirci et al. (2007) evaluated the DPPH$^{\bullet}$ scavenging activity of *C. libanoticum* fruit essential oil, and they reported the IC_{50} value with >30 mg/mL [10]. Kurkcuoglu et al. (2018) found that the essential oil obtained from aerial parts of *C. aromaticum* inhibited DPPH radical by 2.06% at 20 mg/mL [7]. Ebrahimabadi et al. (2010) evaluated the DPPH radical scavenging activity of *C. macropodum* leaf and flower's essential oils and extracts. The results revealed that the extracts had higher activity than the essential oils [23].

3.3. Tyrosinase Inhibition of *C. libanoticum* Oil

Tyrosinase is a rate-limiting enzyme for the biosynthesis of melanocytes. Thus, it is considered the primary target for skin hyperpigmentation disorders. In the present study, tyrosinase inhibition of the essential oil was tested at 1 mg/mL of concentration, and it exhibited considerable effect (Table 3). However, the results were found to be weak when compared to standard, kojic acid. To the best of our knowledge, tyrosinase inhibition of the essential oil of *Chaerophyllum* species was evaluated for the first time.

4. CONCLUSION

According to our findings, the essential oil isolated from the fruits of *C. libanoticum* was rich in monoterpene hydrocarbons and oxygenated monoterpenes. The essential oil possesses moderate antioxidant and antityrosinase activity. The effects were weak when compared with positive controls. activity.

Ethical approval

Not applicable, because this article does not contain any studies with human or animal subjects.

Table 3. Activity results of the essential oil of *C. libanoticum*

	DPPH• scavenging activity %[a]	TEAC[b] (mmol/L)	Tyrosinase inhibition %[b]
C. libanoticum EO	31.3 ± 1.1	0.027 ± 0.008	17.7 ± 1.6
Gallic acid[c]	1.93 ± 0.02	-	-
Ascorbic acid[c]	9.3 ± 0.01	-	-
Kojic acid[c]	-	-	3.6 ± 0.01

Data was given as mean ± SD ($n = 3$) [a] ; Samples tested at 5 mg/mL concentration, [b] ; Samples tested at 1 mg/mL concentration; [c] ; Positive controls, values represented IC_{50}, µg/mL), EO: essential oil

Author contribution

Concept: HGA, BT, MK; Design: HGA, BT, MK; Supervision: KHCB; Materials: AD; Data Collection and/or Processing: MK, BT; Analysis and/or Interpretation: MK, BT; Literature Search: MK, HGA, BT; Writing: BT, MK, HGA, KHCB; Critical Reviews: KHCB.

Source of funding

This research received no grant from any funding agency/sector.

Conflict of interest

The authors declared that there is no conflict of interest.

REFERENCES

1. Sayed-Ahmad B, Talou T, Saad Z, Hijazi A, Merah O. The Apiaceae: Ethnomedicinal family as source for industrial uses. Ind Crops Prod. 2017;109:661-671. https://doi.org/10.1016/j.indcrop.2017.09.027
2. Ngahang Kamte SL, Ranjbarian F, Cianfaglione K, et al. Identification of highly effective antitrypanosomal compounds in essential oils from the Apiaceae family. Ecotoxicol Environ Saf. 2018;156:154-165. https://doi.org/10.1016/j.ecoenv.2018.03.032
3. Davis PH. Flora of Turkey and the East Aegean Islands (Vol. 4). Edinburgh: University Press; 1972. 312-318 p.
4. Zengin G, Sinan KI, Ak G, et al. Chemical profile, antioxidant, antimicrobial, enzyme inhibitory, and cytotoxicity of seven Apiaceae species from Turkey: A comparative study. Ind Crops Prod. 2020;153:112572. https://doi.org/10.1016/j.indcrop.2020.112572
5. Baytop T. A dictionary of vernacular names of wild plants of Turkey (Turkce bitki adları sozlugu–TDK Yayınları), No. 578. Ankara: Publication of the Turkish Language Society; 1994. ISBN: 9751605423.
6. Baser KHC, Tabanca N, Özek T, Demirci B, Duran A, Duman H. Composition of the essential oil of Chaerophyllum aksekiense A. Duran et Duman, a recently described endemic from Turkey. Flavour and Fragr J. 2000;15(1):43-44. https://doi.org/10.1002/(SICI)1099-1026(200001/02)15:1%3C43::AID-FFJ864%3E3.0.CO;2-%23
7. Kurkcuoglu M, Sen A, Bitis L, Birteksoz Tan S, Dogan A, Baser KHC. Chemical composition, anti-inflammatory, antioxidant and antimicrobial activity of essential oil from aerial parts of Chaerophyllum aromaticum L. from Turkey. J Essent Oil-Bear Plants. 2018;21(2):563-569. https://doi.org/10.1080/0972060X.2018.1441748
8. Kurkcuoglu M, Baser KHC, Iscan G, Malyer H, Kaynak G. Composition and anticandidal activity of the essential oil of Chaerophyllum byzantinum Boiss. Flavour and Fragr J. 2006;21(1):115-117. https://doi.org/10.1002/ffj.1539
9. Agalar HG, Altıntas A, Demirci B. The essential oil profiles of chaerophyllum crinitum and C. macrospermum growing wild in Turkey. Nat Volatiles Essent Oils. 2021;8(1):39-48. https://doi.org/10.37929/nveo.871951
10. Demirci B, Kosar M, Demirci F, Dinc M, Baser KHC. Antimicrobial and antioxidant activities of the essential oil of Chaerophyllum libanoticum Boiss. et Kotschy. Food Chem. 2007;105(4):1512-1517. https://doi.org/10.1016/j.foodchem.2007.05.036
11. Ghannadi A, Sajjadi SE, Kukhedan AJ, Mortazavian SM. Volatile constituents of flowering aerial parts of Chaerophyllum macropodum Boiss. from Iran. J Essent Oil-Bear Plants. 2011;14(4):408-412. https://doi.org/10.1080/0972060X.2011.10643594
12. Celikezen FC, Turkoglu V, Fırat M, Bas Z. The Effects of Coriandrum sativum L. and Chaerophyllum macropodum Boiss. (Apiaceae) on human plasma angiotensin-converting enzyme (ACE) in vitro. Bitlis Eren Üniversitesi Fen Bilimleri Dergisi. 2021;10(3):710-718. https://doi.org/10.17798/bitlisfen.894569
13. Coruh N, Sagdıcoglu-Celep AG, Ozgokce F. Antioxidant properties of Prangos ferulacea (L.) Lindl., Chaerophyllum macropodum Boiss. and Heracleum persicum Desf. from Apiaceae family used as food in Eastern Anatolia and their inhibitory effects on glutathione-S-transferase. Food Chem. 2007;100:1237-1242. https://doi.org/10.1016/j.foodchem.2005.12.006

14. Dall'Acqua S, Viola G, Piacente S, Cappelletti EM, Innocenti G. Cytotoxic constituents of roots of Chaerophyllum hirsutum. J Nat Prod. 2004;67:1588-1590. https://doi.org/10.1021/np040046w

15. Saeedi M, Masoumeh E, Khadijeh K. Kojic acid applications in cosmetic and pharmaceutical preparations. Biomed Pharmacother. 2019;110:582-593. https://doi.org/10.1016/j.biopha.2018.12.006

16. Adams RP. Identification of Essential Oil Components by Gas Chromatography/Mass Spectrometry. Carol Stream, IL: Allured Publ. Corp; 2007. ISBN 978-1-932633-11-4.

17. Hochmuth DH. MassFinder-4. Hamburg, Germany: Hochmuth Scientific Consulting; 2008.

18. McLafferty FW, Stauffer DB. The Wiley/NBS Registry of Mass Spectral Data, J.Wiley and Sons: New York; 1989.

19. Curvers J, Rijks J, Cramers C, Knauss K, Larson P. Temperature programmed retention indexes: calculation from isothermal data. Part 1: Theory. J High Resolut Chromatogr. 1985;8:607-610. https://doi.org/10.1002/jhrc.1240080926

20. Agalar HG, Temiz B. HPTLC-DPPH• and HPTLC-tyrosinase methods for hot water-soluble contents of kumquat, limequat and Mexican lime fruit powders. J Res Pharm. 2021;25(5):569-580. https://doi.org/10.29228/jrp.48

21. Re R, Pellegrini N, Proteggente A, Pannala A, Yang M, Rice-Evans C. Antioxidant activity applying an improved ABTS radical cation decolorization assay. Free Radic Biol Med. 1999;26(9-10):1231-1237. https://doi.org/10.1016/S0891-5849(98)00315-3

22. Chizzola R. Composition of the essential oil of Chaerophyllum aromaticum (Apiaceae) growing wild in Austria. Nat Prod Commun. 2009;4(9):1235-1238. https://doi.org/10.1177/1934578X0900400916

23. Ebrahimabadi AH, Djafari-Bidgoli Z, Mazoochi A, Kashi FJ, Batooli H. Essential oils composition, antioxidant and antimicrobial activity of the leaves and flowers of Chaerophyllum macropodum Boiss. Food Control. 2010;21(8):1173-1178. https://doi.org/10.1016/j.foodcont.2010.01.014

ANADOLU UNIVERSITY
INSTITUTE OF HEALTH SCIENCES

European Journal of Life Sciences 2022; 1: 35-41

Review Article

High-density lipoprotein: Quality is more important than quantity!

İpek Ertorun[1], Gülşen Akalın Çiftçi[2], Özkan Alataş[1]

[1]Department of Medicinal Biochemistry, Faculty of Medicine, Eskisehir Osmangazi University, Eskişehir, Turkey.
[2]Department of Biochemistry, Faculty of Pharmacy, Anadolu University, Eskişehir, Turkey.

✉ İpek Ertorun
erdoganipek@gmail.com

https://doi.org/10.55971/EJLS.1099595

Received: 04.06.2022
Accepted: 04.19.2022
Available online: 06.06.2022

ABSTRACT

High density lipoproteins (HDLs) are complex lipid carriers which replace their own structures and functions according to different conditions including healthy or pathological status. HDL has substantial roles in reverse cholesterol transport system for regulation of lipid metabolism. Also HDL has many functions such as antiinflammation, antioxidation, antithrombotic and vasodilator actions. However, these functions may be compromised under pathological conditions. Nowadays, it's known that the function of HDL is more important than it's dose for preventing against cardiovascular diseases. This review mostly summarizes available information of HDL structure, metabolism and the real information related to the physicochemical changes of HDLs causing their different functions. Also HDLs, that lost their protective functions have been associated with oxidative stress and systemic inflammation diseases.

Keywords: Antiinflammatory, antioxidant, dysfunctional HDL, high-density lipoproteins

1. INTRODUCTION

Lipoproteins carry apolar lipids in the center of their structures including cholesterol esters and triglycerides. Also, they have hydrophilic membrane carrying phospholipids, cholesterol, and apolipoproteins. These lipid carriers are grouped according to their size, apolipoproteins and lipid composition. Lipoproteins are grouped as chylomicrons, chylomicron remmants, very low density lipoproteins (VLDL), intermediate density lipoproteins (IDL), low density lipoproteins (LDL), high density lipoproteins (HDL) and Lp(a). Table 1 shows the classification of lipoproteins and the major lipids and major apoproteins that these lipoproteins contain (Table 1) [1,2].

HDLs, which will be discussed, have different roles such as antiinflammatory, antioxidant and reverse cholesterol transport. These roles of HDLs can be observed under both physiological and pathological situations. Such as, HDLs undertake antiinflammatory roles in the immune system when inflammatory conditions occurs and change their structures for carrying proinflammatory molecules [3]. This review reports the novel knowledges linking up the relationships between physicochemical charecteristics of HDLs and those changes found in the pathological circumstantes such as oxidative stress and systemic inflammation.

HDL Structure:

HDLs have complex and heterogeneous structures among other class of lipoproteins by carrying important differences in composition, shape, size and function [4]. HDLs have small (5-17 nm diameter) and most dense (1,063-1,25 g/mL) structures in the

Table 1. Lipoprotein classes

Lipoprotein	Density (g/ml)	Major Lipids	Major Apoproteins
Chylomicrons	<0.930	Triglycerides	Apo B-48, Apo C, Apo E, Apo A-I, A-II, A-IV
Chylomicron Remnants	0.930- 1.006	Triglycerides Cholesterol	Apo B-48, Apo E
VLDL	0.930- 1.006	Triglycerides	Apo B-100, Apo E, Apo C
IDL	1.006- 1.019	Triglycerides Cholesterol	Apo B-100, Apo E, Apo C
LDL	1.019- 1.063	Cholesterol	Apo B-100
HDL	1.063- 1.210	Cholesterol Phospholipids	Apo A-I, Apo A-II, Apo C, Apo E
Lp (a)	1.055- 1.085	Cholesterol	Apo B-100, Apo A

group of lipoproteins. HDLs have different shaped forms such as discoidal (nascent) and sypherical (mature).

Nascent HDL consists of 100 to 150 phospholipid molecules in phospholipid bilayer as found in plasma membrane and 2 to 5 Apo A-1 molecules creating a band around the lipid structure. Nascent HDL contains approximately 10% of overall circulating HDL. Apo A-I and Apo A-II are the most existing protein contents of the nascent HDL. Numerous phospholipids and few triglycerides, free cholesterol and cholesteryl esters are also found in this unique structure. Nascent HDL is converted into mature HDL, that is the main type of HDL in the blood stream [5]. The structure of these mature HDL particle contains of 3–5% cholesterol, approximately 5% triglycerides, 15–20% esterified cholesterol, 26–32% phospholipids and 45–55% apolipoprotein molecules. The lipid core of HDL is consist of cholesterol esters (CE). Apo A-I and Apo A-II are main apoproteins of this mature HDL and few Apo E and Apo C are also found around of lipid structure. HDL is divided into three classes considering their densities: HDL1, HDL2 and HDL3 which have densities of 1,050-1,063 g/ml, 1,063-1,12 g/ml and 1,12-1,21 g/ml respectively.

Moreover, these classes of HDLs are also consists of five different subclasses such as HDL2 and 2b, HDL3a, 3b, and 3c, according to their size. HDL3 which is the first small and mature form of HDL is the best acceptor of free cholesterol. When the amount of esterified free cholesterol increases, the particle size increases and HDL2 occurs. HDL2 is further enhanced by cholesterol esters and also obtain apoE. This apo E-containing particle (HDL1) actually constitute a small fraction of HDL but is known as metabolically active subclass [6,7].

Besides, HDL particles comprise some other components with different biological activity such as vitamins, hormones and microRNAs. HDL succesfully takes these functional miRs to their target cells. Hence, microRNAs consilidate structure of HDL particles [8].

Apo A-I is an effective molecule that contributes in nearly all known functions of HDL particle. Apo A-I provides the coaction of HDL particle with ATP-binding cassette transporters A1 (ABCA1), G1, scavenger receptor B1 and lecithin cholesterol acyltransferase (LCAT) [9]. These cholesterol-phospholipid transporters expressed in hepatocytes, enterocytes, macrophages and other tissues [10]. The main structure of high-density lipoprotein is shown in figure 1.

HDL Metabolism and Function:

Firstly, Apo A-I is synthesized in the metabolism of HDL particles. Nearly 80% of these Apo A-I molecules are obtained by de novo synthesis in hepatocytes and others secreted by intestinal mucosa (20%). The name of this firstly synthesized nascent protein and phospholipid structure is the form of pre-β1 HDL. In blood stream, coaction of Apo A-I or pre-β1 HDL with ABCA1 transporters is an important process for beginning of HDL functions. The Apo A-I also starts activation of LCAT enzyme. These mentioned receptors cause tranportation of phospholipids and free cholesterol from peripheral tissues to HDL particle and transformation of initial particles into nascent HDL (α4 HDL). Cholesteryl esters obtained by LCAT enzyme located with

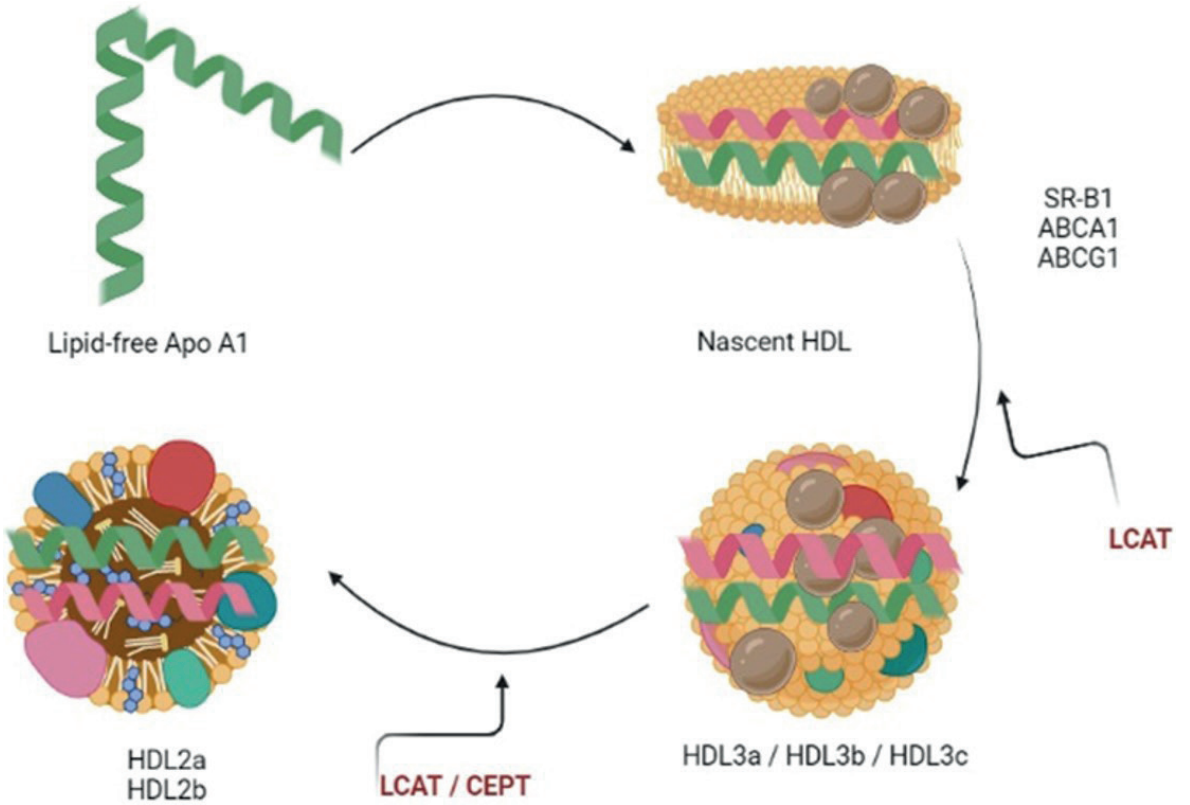

Figure 1. The main structure of high-density lipoprotein

triglycerides in the hydrophobic core of discoidal HDL. Formation of mature HDL structure begins with accumulation of triglycerides and cholesteryl ester. This sypherical HDL form is the main particles in circulation. Conformational changes in this Apo A-I are critical for formation of sypherical HDL and functions for transport of cholesterol from peripherical tissues to HDL. The sypherical HDL is developed by continuous of the LCAT enzyme effect and the activities of lipid transfer proteins. Mature HDL formation is further continued by different proteins such as cholesteryl ester transfer protein (CETP) and the phospholipid transfer protein (PLTP). HDL concentrations and structure are controlled by these proteins in circulation [5]. Another important feature of HDL is that it contains paraoxonase 1 (PON-1) enzyme in its structure [10].

Apo A-I has the HDL associated enzymes PON-1 and platelet activating factor acetylhydrolase (PAF-AH) which suppress LDL oxidation by hyrolizing oxidized lipids [11]. HDL performs multiple physiological functions. Especially HDL is a substantial molecule for continuity of whole lipid metabolism [12]. The most important role of HDL is the continous activity of RCT pathway which removes cholesterol from peripheral tissues to the liver exerting antiatherosclerotic character of this lipoprotein. It is therefore considered an antiatherosclerotic lipoprotein. This process is called the HDL cycle and protects endothelial cells. Actually, HDLs prevent toxic accumulation of cholesterol and cause transformation of cholesterol into bile acids [13]. HDL has roles to interfere with nitric oxide (NO) metabolism because of it's preventive effects on endothelial cells and vascular function. Except that Apo A-I, HDL related enzymes and apolipoproteins such as PON-1 and Apo E stimulate eNOS and increase NO production [14]. Antiinflammatory action of HDL is associated with Apo A-I, PON-1 and sphingosine-1-phosphate contents. HDL prevents migration and infiltration of monocytes and macrophages to the arterial wall by inhibiting monocyte chemoattractant protein 1 (MCP 1) which induced by LDL [15].

The other indispensable role of HDL is its antioxidant action. HDL succeess this action by preventing of lipid oxidation and removing oxidized products. Because of interaction of inflammation and oxidative stress, HDL's antioxidant characteristic contributes to it's antiinflammatory behaviors [6]. Furthermore, HDL has antithrombotic effects because of it's roles on the prostacyclin signaling pathway. It's known that prostacyclins interact with NO to protect against platelet activation and aggregation. HDL also induce the expression of cyclooxygenase 2, that induce prostacyclin synthesis in endothelial cells. Moreover, HDLs protect against apoptosis of endothelial cells by reduction of CPP32-like protease activity, resulting in a decrease in the effect of tumor necrosis factor (TNF-α) [16]. HDL-C physiological functions are shown in figure 2.

To summarize the functions of HDL; HDL transfers apoproteins to other lipoproteins. It takes lipids from other lipoproteins and esterifies cholesterols by the LCAT reaction. By transferring appropriate esters to other lipoproteins, it ensures the transport of cholesterol to the liver. Also, antithrombotic property of HDL is it's ability to induce the generation of prostacyclin. HDL particles are highly antiatherogenic and inhibite endothelial cell apoptosis and prevents against LDL oxidation.

What conditions make HDL go bad?

HDLs obtained from healthy people have frequently antiinflammatory characteristics. On the other hand, when systemic inflammation occurs in organism, HDL can turn into proinflammatory form as part of an acute phase response. Coronary atherosclerosis, surgery, diabetes mellitus, influenza, sepsis, chronic systemic inflammation are a good examples of this effect [17].

Proinflammatory properties of HDL

HDL has an antiinflammatory effect through two mechanisms. 1) Normal HDLs protect LDL-C against oxidation. Then it decrease attraction of monocytes into arterial tissue and occurrance of foam cells that caused by oxidized LDL. 2) Normal HDLs carry out reverse cholesterol transport by removing cholesterol from peripheral tissues.

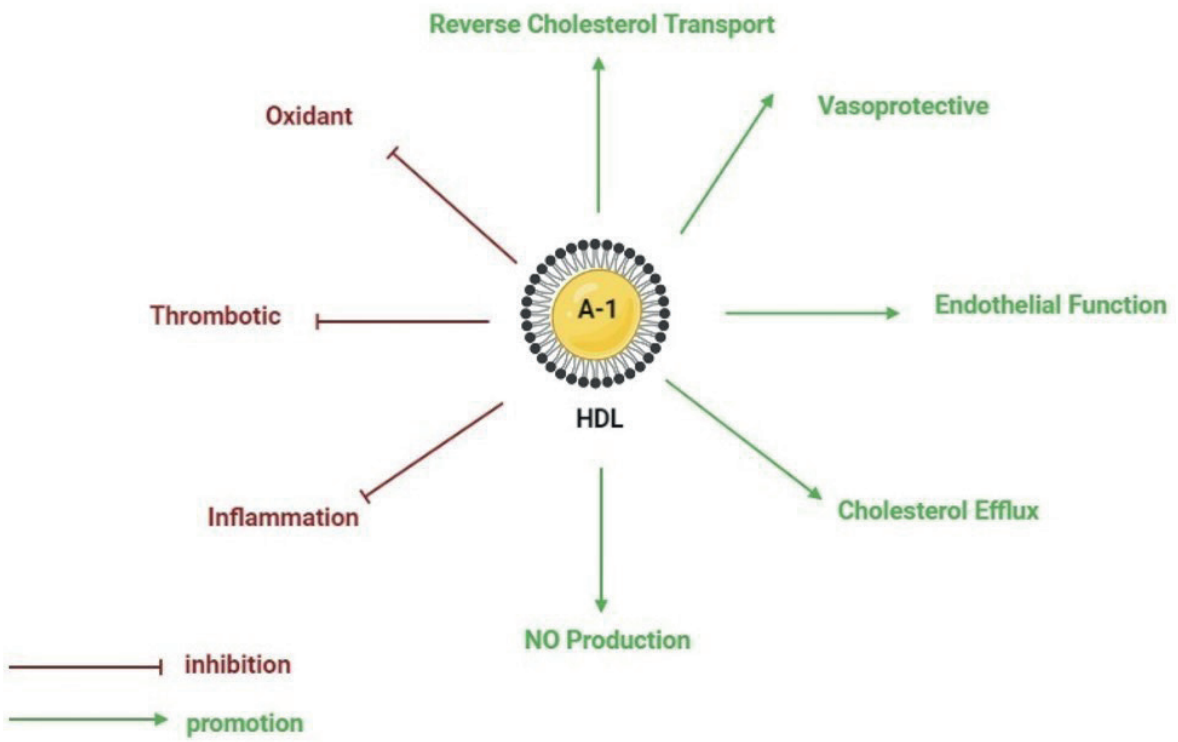

Figure 2. Physiological functions of HDL-C

HDLs have some antioxidant enzymes to work the continuity of an antiinflammatory statement. More than twenty years ago, it was shown that HDL can be in proinflammatory state during an acute phase response in humans and animal after a surgery [18].

During systemic inflammatory state antioxidants can decrease and HDL can increase oxidized lipids and proteins that enhance it's proinflammatory state. Dysfunctional HDL causes releasing of proinflammatory cytokines that evoke transportation of monocytes into arterial walls, which eventually causes to occurance of macrophage accumulation [19]. Atherosclerosis, in its simplest form, is accumulation of oxide LDL-C and triglycerides in peripheral vascular cells. ABCA1 and ABCG1 have roles in prevention and regression of atherosclerosis by removing of excess oxidized cholesterol from macrophages and forming of normal high density lipoprotein [20].

Dysfunctional HDL is also created by myeloperoxidase (MPO). MPO, released from macrophages in atherosclerotic lesions, causes oxidative damage to Apo A-I. It's known that HDLs isolated from the atherosclerotic lesions contain in large quantities of MPO modified proteins such as nitrated and chlorinated Apo A-I [21].

Pro-oxidant properties of HDL

HDL may incorporate lipid peroxidation products and phospholipid containing hydroperoxides that given by oxidized LDL. Furthermore, HDL has roles in hydrolyzing oxidized phospholipids, such as F2-isoprostanes, formed during the oxidative modification of LDL [22]. On the other hand, oxidized HDL may induce the production of reactive oxygen species (ROS) and enhance the risk of cardiovascular diseases by upregulating expression of some proinflammatory genes such as tumor necrosis factor alfa, cyclooxygenase 2 and plasminogen activator inhibitor-1 (PAI-1) [23]. In addition to all this, the enrichment of HDL with triglycerides, MPO, phospholipase A2, ceruloplasmin and serum amyloid A decrease its antioxidant activity and cause the formation of prooxidant HDL [24]. It was shown that oxidized HDLs can not carry out cholesterol efflux from foam cells [25-28].

Methods of HDL Measurement in the Laboratory

Some *in vitro* and *ex vivo* reproducible methods were developed to determine HDL's heterogeneity and various functions. Therewithal detection of the presence of dysfunctional HDL in the patient will help to change the treatment process positively [24]. Standard method for measuring HDL-C; It is the precipitation of lipoproteins using a polyanion such as heparin $MnCl_2$, phosphotungstate $MnCl_2$, dextran sulfate $MnCl_2$ or polyethylene glycol, and then determining the cholesterol value by an enzymatic colorimetric test. These methods have limitations regarding insufficient precipitation of Apo B lipoproteins and assay enviroment that influence HDLC measurement. These insufficiencies could produce inaccurate HDLC measurement for the correct define of cardiovascular risk. On the other hand, electrophoresis, ultracentrifugation, chromatography and nuclear magnetic resonance can be seen more purified methods to separate HDLC in plasma [29]. But this methods have also disadvantages because of requirement of specialized equipment or performing and learning of the methodology is diffucult. Hence, the colorimetric methods are used to measure of HDL composition [30].

The increases or decreases in the change in fluorescence intensity (FI) caused by dichlorofluorescein diacetate (DCFHDA) oxidation can be measured to define the functional characteristics of HDL rather than quantity.

This method measure the capability of various doses of HDL to reduce the generation of intracellular H_2O_2 as reflected by the decrease in the generation of FI by DCF [31] (Figure 3).

2. CONCLUSION

The heterogeneity in the structure and content of HDL is the source of its functional diversity and importance. HDL components and their activity especially in the disease state undergoing significant modifications dynamically change. Such dysfunctional HDL particles appear as both a cause and a symptom of many diseases, especially atherosclerosis. Nowadays, routine lipid measurements in laboratories have

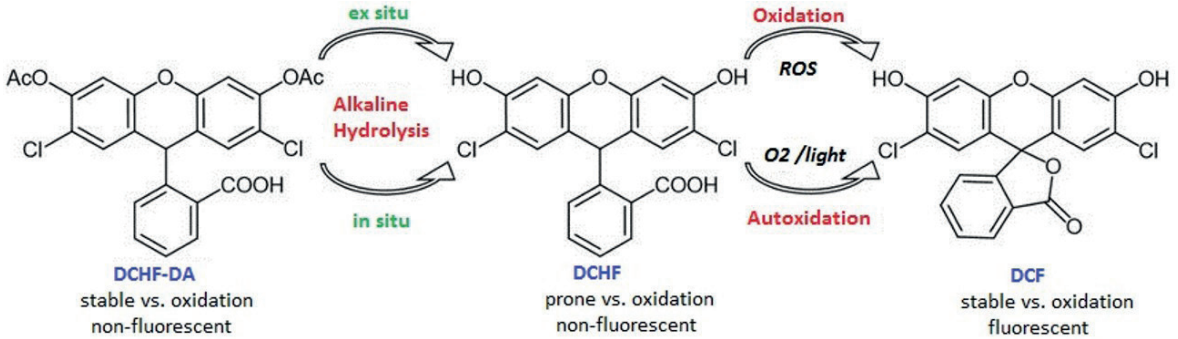

Figure 3. Oxidation of dichlorofluorescein diacetate

become a misleading indicator. In the light of current information, when assessing HDL in the body, It is clear that it is essential to make a qualitative analysis rather than a quantitative one.

ACKNOWLEDGEMENTS

Figures were created with BioRender.com

Author contribution

Concept: IE, GAC, OA; Design: IE and GAC; Supervision: OA; Data Collection and/or Processing: IE and GAC; Literature Search: IE; Writing: IE and GAC; Critical Reviews: IE, GAC and OA.

Source of funding

This research received no grant from any funding agency/sector.

Conflict of interest

The authors declared that there is no conflict of interest.

REFERENCES

1. Namita RC, Jayanta RC. Sleisenger and Fordtran's Gastrointestinal and Liver Disease. 9th ed. 2010. 2410 p. ISBN: 9781416061892.
2. Feingold KR. Introduction to Lipids and Lipoproteins. Endotex. 2021. 1-42 p.
3. Grao-Cruces E, Lopez-Enriquez S, Martin ME, Montserrat-de la Paz S. High-density lipoproteins and immune response: A review. Int J Biol Macromol. 2022;195:117-123. https://doi.org/10.1016/j.ijbiomac.2021.12.009
4. Rothblat GH, Phillips MC. High-density lipoprotein heterogeneity and function in reverse cholesterol transport. Curr Opin Lipidol. 2010;21(3):229-238. https://doi.org/10.1097/mol.0b013e328338472d
5. Ndrepepa G. High-density lipoprotein: a double-edged sword in cardiovascular physiology and pathophysiology. J Lab Precis Med. 2021;6:28. https://doi.org/10.21037/jlpm-21-32
6. Bonizzi A, Piuri G, Corsi F, Cazzola R, Mazzucchelli S. HDL dysfunctionality: Clinical relevance of quality rather than quantity. Biomedicines. 2021;9(7):729. https://doi.org/10.3390/biomedicines9070729
7. Tsompanidi EM, Brinkmeier MS, Fotiadou EH, Giakoumi SM, Kypreos KE. HDL biogenesis and functions: Role of HDL quality and quantity in atherosclerosis. Atherosclerosis. 2010;208(1):3-9. https://doi.org/10.1016/j.atherosclerosis.2009.05.034
8. Ben-Aicha S, Badimon L, Vilahur G. Advances in HDL: Much more than lipid transporters. Int J Mol Sci. 2020;21:732. https://doi.org/10.3390/ijms21030732
9. Vuilleumier N, Dayer JM, von Eckardstein A, Roux-Lombard P. Pro- or anti-inflammatory role of apolipoprotein A-1 in high-density lipoproteins?. Swiss Med Wkly. 2013;143:w13781. https://doi.org/10.4414/smw.2013.13781
10. Bayrak T, Bayrak A, Demirpençe E, Kılınç K. Yeni bir kardiyovasküler belirteç adayı: Paraoksonaz. Hacettepe Tıp Dergisi. 2005;36:147-151.
11. Wang W, Zhou W, Wang B, Zhu H, Ye L, Feng M. Antioxidant effect of apolipoprotein A-I on high-fat diet-inducednon-alcoholic fatty liver disease in rabbits. Acta Biochim Biophys Sin. 2013;45(2):95-103. https://doi.org/10.1093/abbs/gms100

12. Nazir S, Jankowski V, Bender G, Zewinger S, Rye KA, Vorst van EPC. Interaction between high-density lipoproteins and inflammation:Function matters more than concentration. Adv Drug Deliv Rev. 2020;159:94-119. https://doi.org/10.1016/j.addr.2020.10.006

13. Serban MC, Muntean D, Mikhailids DP, Toth PP, Banach M. Dysfunctional HDL: The journey from savior to slayer. Clin Lipidol. 2014;9(1):49-59. https://doi.org/10.2217/clp.13.83

14. Besler C, Heinrich K, Rohrer L, et al. Mechanisms underlying adverse effects of HDL on eNOS-activating pathways in patients with coronary artery disease. J Clin Invest. 2011;121(7):2693-2708. https://doi.org/10.1172/JCI42946

15. Navab M, Imes SS, Hama SY, et al. Monocyte transmigration induced by modification of low density lipoprotein in cocultures of human aortic wall cells is due to induction of monocyte chemotactic protein 1 synthesis and is abolished by high density lipoprotein. J Clin Invest. 1991;88(6):2039-2046. https://doi.org/10.1172/jci115532

16. Pirillo A, Catapano AL, Norata GD. Biological consequences of dysfunctional HDL. Curr Med Chem. 2019;26(9):1644-1664. https://doi.org/10.2174/0929867325666180530110543

17. Ansell BJ. The two faces of the 'good' cholesterol. Cleve Clin J Med. 2007;74(10):697-705. https://doi.org/10.3949/ccjm.74.10.697

18. Van Lenten BJ, Hama SY, de Beer FC, et al. Anti-inflammatory HDL becomes pro-inflammatory during the acute phase response. Loss of protective effect of HDL against LDL oxidation in aortic wall cell cocultures. J Clin Invest. 1995;96(6):2758-2767. https://doi.org/10.1172/jci118345

19. McEneny J, Wade L, Young IS, et al. Lycopene intervention reduces inflammation and improves HDL functionality in moderately overweight middle-aged individuals. J Nutr Biochem. 2013;24(1):163-168. https://doi.org/10.1016/j.jnutbio.2012.03.015

20. Matsuo M. ABCA1 and ABCG1 as potential therapeutic targets for the prevention of atherosclerosis. J Pharmacol Sci. 2022;148:197-203. https://doi.org/10.1016/j.jphs.2021.11.005

21. Kameda T, Horiuchi Y, Shimano S, et al. Effect of myeloperoxidase oxidation and N-homocysteinylation of high-density lipoprotein on endothelial repair function. Biol Chem. 2021;403(3):265-277. https://doi.org/10.1515/hsz-2021-0247

22. Brites F, Martin M, Guillas I, Kontush A. Antioxidative activity of high-density lipoprotein (HDL): Mechanistic insights into potential clinical benefit. BBA Clin. 2017;8:66-77. https://doi.org/10.1016/j.bbacli.2017.07.002

23. Wang Y, Ji L, Jiang R, Zheng L, Liu D. Oxidized high-density lipoprotein induces the proliferation and migration of vascular smooth muscle cells by promoting the production of ROS. J Atheroscler Thromb. 2014;21(3):204-216. https://doi.org/10.5551/jat.19448

24. G HB, Rao VS, Kakkar VV. Friend Turns Foe: Transformation of Anti-Inflammatory HDL to Proinflammatory HDL during Acute-Phase Response. Cholesterol. 2011;2011:274629. https://doi.org/10.1155/2011/274629

25. Khera AV, Cuchel M, de la Llera-Moya M, et al. Cholesterol efflux capacity, high-density lipoprotein function, and atherosclerosis. N Engl J Med. 2011;364(2):127-135. https://doi.org/10.1056/nejmoa1001689

26. Patel PJ, Khera AV, Wilensky RL, Rader DJ. Anti-oxidative and cholesterol efflux capacities of high-density lipoprotein are reduced in ischaemic cardiomyopathy. Eur J Heart Fail. 2013;15(11):1215-1219. https://doi.org/10.1093/eurjhf/hft084

27. Kim K, Shim D, Lee JS, et al. Transcriptome analysis reveals nonfoamy rather than foamy plaque macrophages are proinflammatory in atherosclerotic murine models. Circ Res. 2018;123(10):1127-1142. https://doi.org/10.1161/circresaha.118.312804

28. Ford HZ, Byrne HM, Myerscough MR. A lipid-structured model for macrophage populations in atherosclerotic plaques. J Theor Biol. 2019;479:48-63. https://doi.org/10.1016/j.jtbi.2019.07.003

29. Bitla A, Naresh S, Sachan A. High-density lipoprotein: Quality versus quantity in type 2 diabetes mellitus. J Clin Sci Res. 2019;8(4):193-200. https://doi.org/10.4103/JCSR.JCSR_108_19

30. Cazzola R, Cassani E, Barichella M, Cestaro B. Impaired fluidity and oxidizability of HDL hydrophobic core and amphipathic surface in dyslipidemic men. Metabolism. 2013;62(7):986-991. https://doi.org/10.1016/j.metabol.2013.01.012

31. Yusoff WNW, Bakar NAA, Muid S, Ali AM, Froemming GRA, Nawawi H. Antioxidant activity of high density lipoprotein (HDL) using different in vitro assay. Int J Fundam Appl Sci. 2017;9(6S):298-315. https://doi.org/10.4314/jfas.v9i6s.24